

POLITECNICO DI TORINO
Repository ISTITUZIONALE

Analytic Iterative Solution of Electromagnetic Pulse Coupling to Multiconductor Transmission Lines

Original

Analytic Iterative Solution of Electromagnetic Pulse Coupling to Multiconductor Transmission Lines / Xie, Yan zhao; Guo, Jun; Canavero, Flavio. - In: IEEE TRANSACTIONS ON ELECTROMAGNETIC COMPATIBILITY. - ISSN 0018-9375. - STAMPA. - 55:3(2013), pp. 451-466. [10.1109/TEMC.2013.2242472]

Availability:

This version is available at: 11583/2647376 since: 2016-09-05T13:32:27Z

Publisher:

IEEE

Published

DOI:10.1109/TEMC.2013.2242472

Terms of use:

This article is made available under terms and conditions as specified in the corresponding bibliographic description in the repository

Publisher copyright

(Article begins on next page)

Analytic Iterative Solution of Electromagnetic Pulse Coupling to Multiconductor Transmission Lines

Yan-zhao Xie, Jun Guo, and Flavio G. Canavero

Abstract—This paper provides an efficient iterative solution in the frequency domain for electromagnetic pulse (EMP) radiated field coupling to multiconductor transmission lines (MTLs) based on distributed analytical representation of the exciting sources and iterative technique originated from waveform relaxation. The method consists of two kinds of iterations, the first is that the incoming EMP wave couples to each conductor while the effects of neighboring conductors were neglected; the second is that each conductor will be not only subject to the illumination of the EMP wave, but also influenced by the virtual sources which are the induced voltages and currents of the neighboring conductors at the previous iteration. The key highlights of the proposed method are that the induced voltage and current at each iteration are considered as the virtual distributed exciting sources for next iteration, and the integrals were solved analytically by the Baum–Liu–Teschke equation, leading to a pretty good efficiency and quick convergence for most real cases. The validation results over a wide range show that the proposed method could efficiently handle EMP coupling to MTLs with a large number of conductors and the accuracy of the solutions is closely related to the number of iterations allowing the flexibility to choose between the accuracy and the time cost.

Index Terms—Analytical solution, electromagnetic interference, electromagnetic pulse (EMP), iterative method, transient analysis, transmission line modeling, waveform relaxation (WR).

I. INTRODUCTION

THE electromagnetic pulse produced by high altitude nuclear detonation (HEMP), electro-static discharge electromagnetic pulse (ESD-EMP), lightning EMP (LEMP), or intentional electromagnetic interference (IEMI, e.g., narrow-band high power microwave and ultrawideband EMP) may induce unwanted voltages and currents in the multiconductor transmission lines (MTLs) and then cause serious damage effects to the connected loads of electronic equipments. Therefore, it is of importance to predict such effects in modern electronic circuits by means of the transient simulation of an EMP coupling to MTLs [1]–[7]. The transmission line approximation

method is one of the commonly used ways to calculate the responses of MTLs when illuminated by an electromagnetic pulse plane wave. Normally, one employs the decoupling algorithm (by means of similarity transformation, i.e., the conventional stamp method, see [1], [2]) to convert the set of coupled partial differential equations of MTLs into a set of decoupled single modal equations. Subsequently, the line voltages and currents at the terminals are obtained as a linear combination of the modal variables. However, the use of the decoupling matrix and the transformation to mode quantities back and forth will increase the CPU cost significantly, especially for the simulation of a large number of coupled transmission lines [7]–[9].

Such technical challenges are similar to cases of the crosstalk prediction in MTLs. Many researchers have devoted to this topic. In 2002, Paul provided an *analytical method* to get the symbolic solution of transmission line equations for crosstalk analysis under the weak coupling assumption (WCA) for a three-conductor lossless line in a nonhomogeneous medium [3]. Physically, the voltage and current of the conductor produce electric and magnetic fields that interact with the other adjacent conductors and induce voltages and currents in those conductors. These induced voltages and currents, in turn, should produce electric and magnetic fields that provide a back interaction or second-order effect. The applicability of the WCA method is restricted since the assumption that this back interaction is negligible. In 2010, Y.-Z. Xie *et al.* proposed an approach using the distributed analytical representation and an iterative technique (DARIT) for the crosstalk computation between MTLs [10], which can take into account this back interaction. Henceforth, this approach is named as the DARIT-crosstalk method. This method makes use of the strong points of the WCA method and the idea of the waveform relaxation with transverse partitioning (WR-TP) method [8]–[13], and provides an iterative approach to analyze crosstalk between the lines in an analytical fashion. The validation results show that the DARIT-crosstalk method has advantages over other numerical methods, especially in the aspects of high efficiency, analytic solution and illustrating the factors affecting the crosstalk, etc.

Based on the previous study and the existing difficulties for decoupling the matrix when solving large-scale MTL equations, this paper aims to develop the DARIT-field (for the prediction of field coupling to lines) method and employs the DARIT-field method to the area of EMP radiated field interaction with MTLs. The DARIT-field method starts with the initial state of coupled transmission lines under WCA and employs a Jacobi iteration algorithm which is similar to the WR-TP to update the state of the transmission lines based on the state of the lines at the previous iteration.

Y.-z. Xie and J. Guo are with the State Key Laboratory of Electrical Insulation and Power Equipment, School of Electrical Engineering, Xi'an Jiaotong University, Shaanxi 710049, China (e-mail: yanzhao.xie@gmail.com; gjgjgj@stu.xjtu.edu.cn).

F. G. Canavero is with the Department of Electronics, Politecnico Di Torino, Turin 10129, Italy (e-mail: flavio.canavero@polito.it).

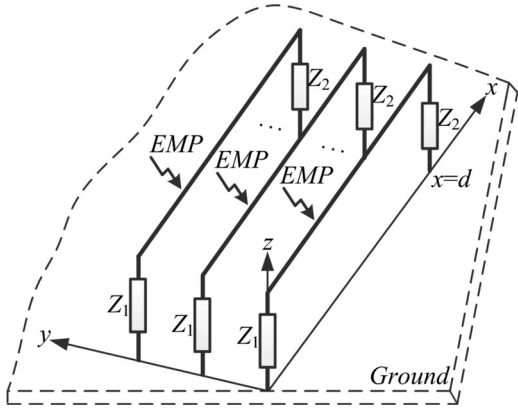


Fig. 1. Configuration of MTLs to be investigated.

The rest of this paper is organized as follows. Section II describes the basic idea of the proposed DARIT-field approach. Section III presents the general terms due to the incoming EMP wave at each iteration. Section IV presents the iterative steps and the derived formulae in detail. Sections V and VI present the validation examples and conclusions, respectively.

II. OUTLINE OF THE PROPOSED APPROACH

The problem to be investigated is shown in Fig. 1. It consists of MTLs of length d and the number of conductors N (the reference conductor is not included), with linear loads at each end of the lines. All the lines are excited by the incoming EMP wave. The EMP wave is first converted to the frequency domain by fast Fourier transform (FFT). Then the formulae are derived in frequency domain. Last, the results in the frequency domain are converted back to the time domain by IFFT. For this problem, the load responses of voltages and currents at each line are to be determined.

A. Basis of the Proposed Algorithm

The Telegrapher's equations of the MTLs in the frequency domain are described by a set of differential equations

$$\begin{aligned} \frac{d\mathbf{V}(x, s)}{dx} + \mathbf{Z}'(s)\mathbf{I}(x, s) &= \mathbf{V}'(x, s) \\ \frac{d\mathbf{I}(x, s)}{dx} + \mathbf{Y}'(s)\mathbf{V}(x, s) &= \mathbf{I}'(x, s) \end{aligned} \quad (1)$$

where $\mathbf{V}(x, s)$ and $\mathbf{I}(x, s)$ are the vectors of the N voltages and currents on the lines. $\mathbf{V}'(x, s)$ and $\mathbf{I}'(x, s)$ are the source terms that detailed expressions depending upon the coupling model used, e.g., the Taylor model (adopted in this paper), the Agrawal model, and the Rachidi model [14]. \mathbf{Z}' and \mathbf{Y}' are the $N \times N$ matrices of the line impedances and admittances that, in general, are frequency dependent and can be written as

$$\mathbf{Z}'(s) = \mathbf{R}'(s) + j\omega\mathbf{L}'(s), \quad \mathbf{Y}'(s) = \mathbf{G}'(s) + j\omega\mathbf{C}'(s). \quad (2)$$

Equations in (1) for line i could be expressed as follows:

$$\begin{aligned} \frac{dv_i(x, s)}{dx} + z'_{ii}(s)i_i(x, s) &= - \sum_{\substack{j=1 \\ j \neq i}}^N z'_{ij}(s)i_j(x, s) + V'_i(x, s) \\ \frac{di_i(x, s)}{dx} + y'_{ii}(s)v_i(x, s) &= - \sum_{\substack{j=1 \\ j \neq i}}^N y'_{ij}(s)v_j(x, s) + I'_i(x, s). \end{aligned} \quad (3)$$

where $V'_i(x, s)$ and $I'_i(x, s)$ are the general source terms of line i due to the incoming EMP wave. The summation terms in (3) are the neighboring effects on line i due to the coupling of other adjacent lines. By applying WR techniques to (3), we obtain a recursive set of decoupled differential equations in the frequency domain

$$\begin{aligned} \frac{dv_i^{(r+1)}(x, s)}{dx} + z'_{ii}(s)i_i^{(r+1)}(x, s) &= e_i^{(r)}(x, s) \\ \frac{di_i^{(r+1)}(x, s)}{dx} + y'_{ii}(s)v_i^{(r+1)}(x, s) &= q_i^{(r)}(x, s) \end{aligned} \quad (4)$$

where r represents the r th iteration, $r \geq 0$. Depending upon where the exciting source comes from, the source terms of the coupling equations $e_i^{(r)}(x, s)$ and $q_i^{(r)}(x, s)$ could be divided by two parts

$$\begin{aligned} e_i^{(r)}(x, s) &= e_{A,i}^{(r)}(x, s) + e_{B,i}^{(r)}(x, s) \\ q_i^{(r)}(x, s) &= q_{A,i}^{(r)}(x, s) + q_{B,i}^{(r)}(x, s). \end{aligned} \quad (5)$$

The first part 'A' ($e_{A,i}^{(r)}$ and $q_{A,i}^{(r)}$) is *neighboring* effects due to the influence of the adjacent lines, which would be updated at each iteration

$$\begin{aligned} e_{A,i}^{(r)}(x, s) &= - \sum_{\substack{j=1 \\ j \neq i}}^N z'_{ij}(s)i_j^{(r)}(x, s) \\ q_{A,i}^{(r)}(x, s) &= - \sum_{\substack{j=1 \\ j \neq i}}^N y'_{ij}(s)v_j^{(r)}(x, s). \end{aligned} \quad (6)$$

The second part 'B' ($e_{B,i}^{(r)}$ and $q_{B,i}^{(r)}$) is the *general* terms due to the excitation of the incoming EMP wave that would remain of the same form at each iteration

$$e_{B,i}^{(r)}(x, s) = V'_i(x, s), \quad q_{B,i}^{(r)}(x, s) = I'_i(x, s). \quad (7)$$

The first iteration in the DARIT-field method is to deal with the incoming EMP wave interacting with each line independently rather than the lumped source propagating along the generator line in the DARIT-crosstalk method. At the second iteration and after, each line will be illuminated by the voltages and currents along the other adjacent lines that are obtained at the previous iteration, and the incoming EMP wave as well. At each iteration, the effects of the adjacent lines are considered as equivalent distributed sources over the lines, and the distribution of the voltages and currents along the line could

be deduced by an analytical expression by means of combined voltage wave proposed by Dr. C. E. Baum when developing the BLT equation [15]. Particularly, the integral of the equivalent distributed sources could be implemented analytically; thus, the time-consuming numerical integration is avoided. The voltages and currents at the terminals (voltages and currents $(v(0), i(0))$ at near ends and $(v(d), i(d))$ at far ends) and the combined voltage wave $(w(0))_+, (w(d))_-$ are solved by the BLT equation at each iteration (see Appendix A in [10]). Therefore, prior to solving the BLT equation, one needs first to get the source vector $\mathbf{W}^{s,(r)}$ as input parameters for the BLT equation calculation

$$\mathbf{W}^{s,(r)} = [w_1^s; \quad w_2^s] \quad (8)$$

where

$$\begin{aligned} w_1^s &= \int_0^d e^{-\gamma_i(d-x')} (w_i^{s,(r)}(x', s))_+ dx' = w_{1,A}^s + w_{1,B}^s \\ w_2^s &= - \int_0^d e^{-\gamma_i x'} (w_i^{s,(r)}(x', s))_- dx' = w_{2,A}^s + w_{2,B}^s \end{aligned} \quad (9)$$

and

$$\begin{aligned} (w_i^{s,(r)}(x, s))_+ &= e_i^{(r)}(x, s) + z_{c,i} q_i^{(r)}(x, s) \\ &= (w_{A,i}^{s,(r)}(x, s))_+ + (w_{B,i}^{s,(r)}(x, s))_+ \\ (w_i^{s,(r)}(x, s))_- &= e_i^{(r)}(x, s) - z_{c,n} q_i^{(r)}(x, s) \\ &= (w_{A,i}^{s,(r)}(x, s))_- + (w_{B,i}^{s,(r)}(x, s))_- \end{aligned} \quad (10)$$

The notation of the Laplace transform variable s in the remaining parts is omitted to abbreviate the length of formulae.

We know that (5) are functions of the distance x from the near end. These terms as new *distributed* source terms for the $(r+1)$ th iteration, $e_i^{(r)}(x, s)$ and $q_i^{(r)}(x, s)$ could be thought of as equivalent *distributed* per-unit-length (p.u.l.) virtual voltage and current sources located along the length of the line i .

The DARIT-crosstalk method [10] has shown that summation terms of the virtual exciting sources in (5) could be expressed in the form of combinations of exponential functions, which is a very good feature to solve the integral analytically. Later, the exciting source due to the incoming EMP wave could also be expressed in the form of exponential functions since the mathematical description of the EMP waveform is a combination of double exponentials.

B. Major Steps at Each Iteration

The major steps at each iteration are listed as follows:

- 1) get the analytic expression of the excitation sources;
- 2) get the expression distribution of the voltage v and the current i as a function of x ;
- 3) evaluate the integrals analytically; and
- 4) compute $w(0)$, $w(d)$ and $(w(0))_+$ and $(w(d))_-$ by means of the BLT equation.

The crucial step is to get the distribution of the voltages and currents as a function of the location on *each line* based on the updated results.

III. DERIVATION OF THE GENERAL ITERATIVE PROCEDURE OF THE INCOMING EMP WAVE

Suppose that the only exciting source is from the incoming EMP wave and the summation terms are zeros. Considering the reflection of the earth to the incoming EMP wave and the selected TL model (here is the Taylor model), the exciting sources in (4) are derived and given as follows:

$$\begin{aligned} e_i^{(0)}(x) &= e_{B,i}^{(0)}(x) = f_v e^{-jkx \cos \psi \cos \phi} \\ q_i^{(0)}(x) &= q_{B,i}^{(0)}(x) = f_i e^{-jkx \cos \psi \cos \phi} \end{aligned} \quad (11)$$

where f_v and f_i are the coefficients given in Appendix A.

The corresponding combined source waves are

$$\begin{aligned} (w_{B,i}^s(x))_+ &= (f_v + z_{c,i} f_i) e^{-jkx \cos \psi \cos \phi} \\ (w_{B,i}^s(x))_- &= (f_v - z_{c,i} f_i) e^{-jkx \cos \psi \cos \phi}. \end{aligned} \quad (12)$$

The two elements of the source vector are derived as follows:

$$\begin{aligned} w_{1,B}^s &= \frac{(f_v + z_{c,i} f_i) e^{-\gamma_i d}}{\gamma_i - jk \cos \psi \cos \phi} \left(e^{(\gamma_i - jk \cos \psi \cos \phi)d} - 1 \right) \\ w_{2,B}^s &= \frac{(f_v - z_{c,i} f_i) e^{-\gamma_i d}}{\gamma_i + jk \cos \psi \cos \phi} \left(e^{-(\gamma_i + jk \cos \psi \cos \phi)d} - 1 \right). \end{aligned} \quad (13)$$

At each iteration, the contribution of the incoming exciting EMP wave would keep the same form as in (13). Based on the calculated results at the terminals, the distribution of voltages and currents due to the exciting EMP wave at each iteration could be derived as follows:

$$\begin{aligned} v_{B,i}^{(r)}(x) &= 0.5 \left(\left(w_i^{(r)}(0) \right)_+ - \frac{(f_v + z_{c,i} f_i)}{\gamma_i - jk \cos \psi \cos \phi} \right) e^{-\gamma_i x} \\ &\quad + 0.5 \left(\left(w_i^{(r)}(d) \right)_- e^{-\gamma_i d} \right. \\ &\quad \left. + \frac{(f_v - z_{c,i} f_i) e^{-(\gamma_i + jk \cos \psi \cos \phi)d}}{\gamma_i + jk \cos \psi \cos \phi} \right) e^{\gamma_i x} \\ &\quad + 0.5 \left(\frac{(f_v + z_{c,i} f_i)}{\gamma_i - jk \cos \psi \cos \phi} \right. \\ &\quad \left. - \frac{(f_v - z_{c,i} f_i)}{\gamma_i + jk \cos \psi \cos \phi} \right) e^{-jk \cos \psi \cos \phi x} \\ &= f_{B,v_1}^{(r)}(i) e^{-\gamma_i x} + f_{B,v_2}^{(r)}(i) e^{\gamma_i x} + f_{B,v_3}^{(r)}(i) e^{-jk \cos \psi \cos \phi x} \\ i_{B,i}^{(r)}(x) &= \frac{0.5}{z_{c,i}} \left(\left(w_i^{(r)}(0) \right)_+ - \frac{(f_v + z_{c,i} f_i)}{\gamma_i - jk \cos \psi \cos \phi} \right) e^{-\gamma_i x} \\ &\quad - \frac{0.5}{z_{c,i}} \left(\left(w_i^{(r)}(d) \right)_- e^{-\gamma_i d} \right. \\ &\quad \left. + \frac{(f_v - z_{c,i} f_i) e^{-(\gamma_i + jk \cos \psi \cos \phi)d}}{\gamma_i + jk \cos \psi \cos \phi} \right) e^{\gamma_i x} \\ &\quad + \frac{0.5}{z_{c,i}} \left(\frac{(f_v + z_{c,i} f_i)}{\gamma_i - jk \cos \psi \cos \phi} \right. \\ &\quad \left. - \frac{(f_v - z_{c,i} f_i)}{\gamma_i + jk \cos \psi \cos \phi} \right) e^{-jk \cos \psi \cos \phi x} \\ &= f_{B,i_1}^{(r)}(i) e^{-\gamma_i x} + f_{B,i_2}^{(r)}(i) e^{\gamma_i x} + f_{B,i_3}^{(r)}(i) e^{-jk \cos \psi \cos \phi x} \end{aligned} \quad (14)$$

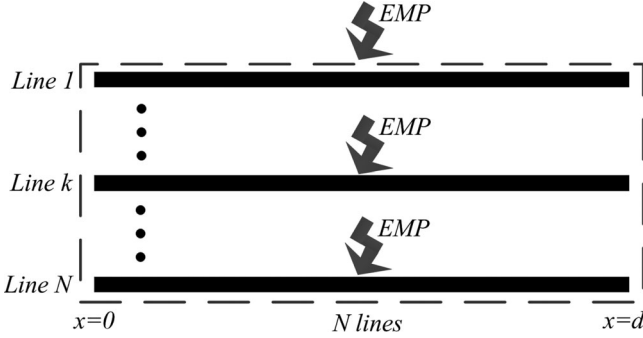


Fig. 2. Diagram of iteration 1.

where γ_i is the propagation constant of line i ; $z_{c,i}$ is the characteristics impedance of line i ; and d is the line length. The expressions of γ_i and $z_{c,i}$ are given as follow:

$$\gamma_i = \sqrt{z_{ii}y_{ii}}, \quad z_{c,i} = \sqrt{z_{ii}/y_{ii}}. \quad (15)$$

IV. MATHEMATICAL DERIVATION OF THE PROPOSED DARIT-FIELD ALGORITHM

We present the derived formulae of four iterations. In order to make a distinction between each iteration, the general subscript indices at these four iterations are denoted by m , n , p , and q , respectively. BLT equation is used to solve the voltages and currents at the terminals. The main task of each iteration is to determine the source vector and the distribution of induced voltage and current along the line.

A. Iteration 1

The diagram of this step is shown in Fig. 2, in which the general subscript index is m . At this iteration, there are no coupling effects from the neighboring line since the initial states of the lines are all zeros. The only exciting source is from the incoming EMP wave. Therefore, (4) could be simplified as

$$\begin{aligned} \frac{dv_m^{(1)}(x, s)}{dx} + z'_{mm}(s)i_m^{(1)}(x, s) &= V'_m(x, s) \\ \frac{di_m^{(1)}(x, s)}{dx} + y'_{mm}(s)v_m^{(1)}(x, s) &= I'_m(x, s). \end{aligned} \quad (16)$$

The two elements w_1^s and w_2^s of the source vector are used in the BLT equation, which are equal to (13) except that the general subscript index is replaced by m . The load responses could be solved in terms of the BLT equation. The distribution of voltage and current along the line could be expressed analytically (the same as in (14) except that the index i replaced by m) and by which to form the virtual exciting sources (part A of the exciting sources) for the next iteration.

B. Iteration 2

The schematic diagram is shown in Fig. 3. As can be seen, hereafter, each line is excited by the incoming EMP wave and the coupling effects of all the other adjacent lines. For the voltages

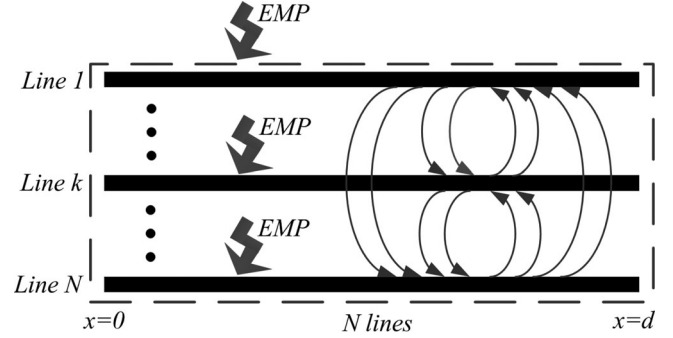


Fig. 3. Diagram of/after Iteration 2 (each line is excited by all the adjacent lines and the incoming EMP wave).

and currents on the n th line, we have

$$\begin{aligned} \frac{dv_n^{(2)}(x)}{dx} + z'_{nn}i_n^{(2)}(x) &= - \sum_{\substack{m=1 \\ m \neq n}}^N z'_{nm}i_m^{(1)}(x) + V'_n(x) \\ \frac{di_n^{(2)}(x)}{dx} + y'_{nn}v_n^{(2)}(x) &= - \sum_{\substack{m=1 \\ m \neq n}}^N y'_{nm}v_m^{(1)}(x) + I'_n(x). \end{aligned} \quad (17)$$

The virtual p.u.l. distributed voltage and current sources due to the effects of adjacent lines are

$$\begin{aligned} e_{A,n}^{(2)}(x) &= - \sum_{\substack{m=1 \\ m \neq n}}^N z'_{nm}i_m^{(1)}(x) \\ &= - \sum_{\substack{m=1 \\ m \neq n}}^N z'_{nm}f_{B,i_1}^{(1)}(j)e^{-\gamma_m x} - \sum_{\substack{m=1 \\ m \neq n}}^N z'_{nm}f_{B,i_2}^{(1)}(m)e^{\gamma_m x} \\ &\quad - \sum_{\substack{m=1 \\ m \neq n}}^N z'_{nm}f_{B,i_3}^{(1)}(m)e^{-jk \cos \psi \cos \phi x} \\ q_{A,n}^{(2)}(x) &= - \sum_{\substack{m=1 \\ m \neq n}}^N y'_{nm}v_m^{(1)}(x) \\ &= - \sum_{\substack{m=1 \\ m \neq n}}^N y'_{nm}f_{B,v_1}^{(1)}(m)e^{-\gamma_m x} - \sum_{\substack{m=1 \\ m \neq n}}^N y'_{nm}f_{B,v_2}^{(1)}(m)e^{\gamma_m x} \\ &\quad - \sum_{\substack{m=1 \\ m \neq n}}^N y'_{nm}f_{B,v_3}^{(1)}(m)e^{-jk \cos \psi \cos \phi x}. \end{aligned} \quad (18)$$

During the iterating procedure, the symmetry of the MTLs, which indicates whether the propagation constants of one line equals to the other's, should be considered. To abbreviate the length of formulae, we use the notations as follows:

$$\begin{aligned} K_{n+,m+} &= \frac{e^{(\gamma_n + \gamma_m)d} - 1}{\gamma_n + \gamma_m} & K_{n+,m-} &= \frac{e^{(\gamma_n - \gamma_m)d} - 1}{\gamma_n - \gamma_m} \\ K_{n-,m+} &= \frac{e^{(\gamma_m - \gamma_n)d} - 1}{\gamma_m - \gamma_n} & K_{n-,m-} &= \frac{e^{(-\gamma_n - \gamma_m)d} - 1}{-\gamma_n - \gamma_m} \end{aligned}$$

$$\begin{aligned}
K_{n+} &= \frac{e^{-(\gamma_n + jk \cos \psi \cos \phi)d} - 1}{-(\gamma_n + jk \cos \psi \cos \phi)} \\
K_{n-} &= \frac{e^{(\gamma_n - jk \cos \psi \cos \phi)d} - 1}{\gamma_n - jk \cos \psi \cos \phi} \\
B_l^{(r+1)+}(n, m) &= (z'_{nm} f_{i_l}^{(r)}(m) + z_{c,n} y'_{nm} f_{v_l}^{(r)}(m)) \\
B_l^{(r+1)-}(n, m) &= (z'_{nm} f_{i_l}^{(r)}(m) - z_{c,n} y'_{nm} f_{v_l}^{(r)}(m))
\end{aligned} \quad (19)$$

where γ_n and γ_m are the propagation constants for line n and m , respectively. The elements of the source vector due to part A are

$$\begin{aligned}
w_{1,A}^s &= e^{-\gamma_n d} \left[- \sum_{\substack{m=1 \\ m \neq n}}^N \left(B_1^{(2)+}(n, m) K_{11}^{(2)} \right. \right. \\
&\quad \left. \left. + B_2^{(2)+}(n, m) K_{n+,m+} + B_3^{(2)+}(n, m) K_{n+} \right) \right] \\
w_{2,A}^s &= \sum_{\substack{m=1 \\ m \neq n}}^N \left(B_1^{(2)-}(n, m) K_{n-,m-} \right. \\
&\quad \left. + B_2^{(2)-}(n, m) K_{21}^{(2)} + B_3^{(2)-}(n, m) K_{n-} \right). \quad (20)
\end{aligned}$$

The values of $K_{11}^{(2)}$ and $K_{21}^{(2)}$ are determined depending upon the symmetry as follows.

1) Unsymmetrical Cases of MTLs ($\gamma_n \neq \gamma_m$):

$$K_{11}^{(2)} = K_{n+,m-}, \quad K_{21}^{(2)} = K_{n-,m+}. \quad (21)$$

2) Symmetrical Cases of MTLs ($\gamma_n = \gamma_m$, the Case of $n = m$ Included):

$$K_{11}^{(2)} = d, \quad K_{21}^{(2)} = d. \quad (22)$$

The exciting sources due to the incoming EMP wave keep the same form as in Section III, but index changes to n

$$e_{B,n}^{(2)}(x) = V'_n(x), \quad q_{B,n}^{(2)}(x) = I'_n(x). \quad (23)$$

The elements of source vector due to part B keep the same form as in (13) except that index changes to n . The two elements of the source vector in the expression of (9) are all obtained at this iteration. The load responses could be solved by the BLT equation. Incorporating the terminal conditions, the voltage $v_n(x)$ and current $i_n(x)$ on line n can be obtained as well. They have the form of exponential function combinations for unsymmetrical cases or more terms in the form of the distance from terminals multiplied by exponential functions for symmetrical cases, which are given by

$$\begin{aligned}
v_n^{(2)}(x) &= f_{v_1}^{(2)}(n) e^{-\gamma_n x} + f_{v_2}^{(2)}(n) e^{\gamma_n x} \\
&\quad + f_{v_3}^{(2)}(n) e^{-jk \cos \psi \phi x} + \sum_{\substack{m=1 \\ m \neq n}}^N \left(f_{v_4}^{(2)}(n, m) e^{-\gamma_m x} \right. \\
&\quad \left. + f_{v_5}^{(2)}(n, m) e^{\gamma_m x} \right) + f_{v_6}^{(2)}(n) x e^{-\gamma_n x} + f_{v_7}^{(2)}(n) x e^{\gamma_n x}
\end{aligned} \quad (24a)$$

$$\begin{aligned}
i_n^{(2)}(x) &= f_{i_1}^{(2)}(n) e^{-\gamma_n x} + f_{i_2}^{(2)}(n) e^{\gamma_n x} \\
&\quad + f_{i_3}^{(2)}(n) e^{-jk \cos \psi \phi x} + \sum_{\substack{m=1 \\ m \neq n}}^N \left(f_{i_4}^{(2)}(n, m) e^{-\gamma_m x} \right. \\
&\quad \left. + f_{i_5}^{(2)}(n, m) e^{\gamma_m x} \right) + f_{i_6}^{(2)}(n) x e^{-\gamma_n x} + f_{i_7}^{(2)}(n) x e^{\gamma_n x}
\end{aligned} \quad (24b)$$

where $f_{v_{1-7}}^{(2)}, f_{i_{1-7}}^{(2)}$ are the predefined coefficients given in Appendix A depending upon whether the case is symmetrical or not.

C. Iteration 3

The diagram is the same as in Iteration 2 (shown in Fig. 3). The Telegrapher's equations for this step are the same as in Iteration 2, but the indices n and m are replaced by p and n , respectively. The virtual p.u.l. distributed voltage and current sources due to the adjacent lines are

$$e_{A,p}^{(3)}(x) = - \sum_{\substack{n=1 \\ n \neq p}}^N z'_{pn} i_n^{(2)}(x), \quad q_{A,p}^{(3)}(x) = - \sum_{\substack{n=1 \\ n \neq p}}^N y'_{pn} v_n^{(2)}(x). \quad (25)$$

The w_1^s and w_2^s used in the BLT equation are derived as follows:

$$\begin{aligned}
w_{1,A}^s &= e^{-\gamma_p d} \left\{ - \sum_{\substack{n=1 \\ n \neq p}}^N \left[B_1^{(3)+}(p, n) K_{11}^{(3)} + B_2^{(3)+}(p, n) K_{p+,n+} \right. \right. \\
&\quad \left. \left. + B_3^{(3)+}(p, n) K_{p+} + B_6^{(3)+}(p, n) K_{12}^{(3)} \right. \right. \\
&\quad \left. \left. + B_7^{(3)+}(p, n) \left(\frac{de^{\gamma_{p,n}^+ d}}{\gamma_{p,n}^+} - \frac{e^{\gamma_{p,n}^+ d} - 1}{(\gamma_{p,n}^+)^2} \right) \right. \right. \\
&\quad \left. \left. + \sum_{\substack{m=1 \\ m \neq n}}^N \left(B_4^{(3)+}(p, n, m) K_{13}^{(3)} + B_5^{(3)+}(p, n, m) K_{p+,m+} \right) \right] \right\} \\
w_{2,A}^s &= \sum_{\substack{n=1 \\ n \neq p}}^N \left[B_1^{(3)-}(p, n) K_{p-,n-} + B_2^{(3)-}(p, n) K_{21}^{(3)} \right. \\
&\quad \left. + B_3^{(3)-}(p, n) K_{p-} + B_7^{(3)-}(p, n) K_{22}^{(3)} \right. \\
&\quad \left. + B_6^{(3)-}(p, n) \left(\frac{de^{-\gamma_{p,n}^+ d}}{-\gamma_{p,n}^+} - \frac{e^{-\gamma_{p,n}^+ d} - 1}{(\gamma_{p,n}^+)^2} \right) \right. \\
&\quad \left. + \sum_{\substack{m=1 \\ m \neq n}}^N \left(B_4^{(3)-}(p, n, m) K_{p-,m-} + B_5^{(3)-}(p, n, m) K_{23}^{(3)} \right) \right]
\end{aligned} \quad (26)$$

where $\gamma_{p,n}^+$, $\gamma_{p,n}^-$, and $B_l^{(3)}(p, n, m)$ are given by

$$\begin{aligned}
\gamma_{p,n}^+ &= \gamma_p + \gamma_n, \quad \gamma_{p,n}^- = \gamma_p - \gamma_n, \\
B_l^{(3)+}(p, n, m) &= (z'_{pn} f_{i_l}^{(2)}(m) + z_{c,n} y'_{pn} f_{v_l}^{(2)}(m)) \\
B_l^{(3)-}(p, n, m) &= (z'_{pn} f_{i_l}^{(2)}(m) - z_{c,n} y'_{pn} f_{v_l}^{(2)}(m)). \quad (27)
\end{aligned}$$

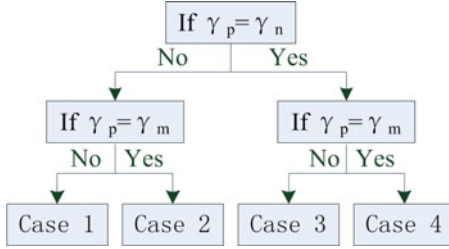


Fig. 4. Symmetry structure of Iteration 3.

Depending upon the symmetry or not (see Fig. 4), $K_{11}^{(3)}$, $K_{12}^{(3)}$, $K_{13}^{(3)}$, and $K_{21}^{(3)}$, $K_{22}^{(3)}$, $K_{23}^{(3)}$ are determined as follows.

Case 1 For $(\gamma_p \neq \gamma_n)$ and $(\gamma_p \neq \gamma_m)$:

$$\begin{aligned} K_{11}^{(3)} &= K_{p+,n-} & K_{21}^{(3)} &= K_{n+,p-} \\ K_{12}^{(3)} &= \frac{de^{\gamma_{p,n}^- d}}{\gamma_{p,n}^-} - \frac{e^{\gamma_{p,n}^- d} - 1}{(\gamma_{p,n}^-)^2} \\ K_{22}^{(3)} &= \frac{de^{\gamma_{n,p}^- d}}{\gamma_{n,p}^-} - \frac{e^{\gamma_{n,p}^- d} - 1}{(\gamma_{n,p}^-)^2}. \\ K_{13}^{(3)} &= K_{p+,m-}, \quad K_{23}^{(3)} = K_{m+,p-}. \end{aligned} \quad (28)$$

Case 2 For $(\gamma_p \neq \gamma_n)$ and $(\gamma_p = \gamma_m)$:

$$\begin{aligned} K_{11}^{(3)} &= K_{p+,n-} & K_{21}^{(3)} &= K_{n+,p-} \\ K_{12}^{(3)} &= \frac{de^{\gamma_{p,n}^- d}}{\gamma_{p,n}^-} - \frac{e^{\gamma_{p,n}^- d} - 1}{(\gamma_{p,n}^-)^2} \\ K_{22}^{(3)} &= \frac{de^{\gamma_{n,p}^- d}}{\gamma_{n,p}^-} - \frac{e^{\gamma_{n,p}^- d} - 1}{(\gamma_{n,p}^-)^2}. \\ K_{13}^{(3)} &= d, \quad K_{23}^{(3)} = d. \end{aligned} \quad (29)$$

Case 3 For $(\gamma_p = \gamma_n)$ and $(\gamma_p \neq \gamma_m)$:

$$\begin{aligned} K_{11}^{(3)} &= d, \quad K_{21}^{(3)} = d, \quad K_{12}^{(3)} = d^2/2 \\ K_{22}^{(3)} &= d^2/2, \quad K_{13}^{(3)} = K_{p+,m-}, \quad K_{23}^{(3)} = K_{m+,p-}. \end{aligned} \quad (30)$$

Case 4 For $(\gamma_p = \gamma_n)$ and $(\gamma_p = \gamma_m)$:

$$\begin{aligned} K_{11}^{(3)} &= d, \quad K_{21}^{(3)} = d, \quad K_{12}^{(3)} = d^2/2 \\ K_{22}^{(3)} &= d^2/2, \quad K_{13}^{(3)} = d, \quad K_{23}^{(3)} = d. \end{aligned} \quad (31)$$

The elements of source vector due to part B are the same as in (13) except for the index. So far, the source vector in (9) at this iteration are derived for the BLT equation. The voltage and current on line p are expressed by $v_p(x)$ and $i_p(x)$, respectively. Although they are in the form of combinations of exponential functions like in Iteration 2, they require more careful analysis since the more complicated terms $x^2 e^{-\gamma_p x}$ and $x^2 e^{\gamma_p x}$ appear in the equations, which are given as follows:

$$\begin{aligned} v_p^{(3)}(x) &= f_{v_1}^{(3)}(p)e^{-\gamma_p x} + f_{v_2}^{(3)}(p)e^{\gamma_p x} + f_{v_3}^{(3)}(p)e^{-jk \cos \psi \cos \phi x} \\ &\quad + f_{v_6}^{(3)}(p)xe^{-\gamma_p x} + f_{v_7}^{(3)}(p)xe^{\gamma_p x} + f_{v_8}^{(3)}(p)x^2 e^{-\gamma_p x} \\ &\quad + f_{v_9}^{(3)}(p)x^2 e^{\gamma_p x} + \sum_{\substack{n=1 \\ n \neq p}}^N \left[f_{v_{10}}^{(3)}(p,n)e^{-\gamma_n x} \right. \\ &\quad \left. + f_{v_{11}}^{(3)}(p,n)e^{\gamma_n x} + f_{v_{12}}^{(3)}(p,n)xe^{-\gamma_n x} + f_{v_{13}}^{(3)}(p,n)xe^{\gamma_n x} \right. \\ &\quad \left. + \sum_{\substack{m=1 \\ m \neq n}}^N \left(f_{v_4}^{(3)}(p,n,m)e^{-\gamma_m x} + f_{v_5}^{(3)}(p,n,m)e^{\gamma_m x} \right) \right] \\ i_p^{(3)}(x) &= f_{i_1}^{(3)}(p)e^{-\gamma_p x} + f_{i_2}^{(3)}(p)e^{\gamma_p x} + f_{i_3}^{(3)}(p)e^{-jk \cos \psi \cos \phi x} \\ &\quad + f_{i_6}^{(3)}(p)xe^{-\gamma_p x} + f_{i_7}^{(3)}(p)xe^{\gamma_p x} + f_{i_8}^{(3)}(p)x^2 e^{-\gamma_p x} \\ &\quad + f_{i_9}^{(3)}(p)x^2 e^{\gamma_p x} + \sum_{\substack{n=1 \\ n \neq p}}^N \left[f_{i_{10}}^{(3)}(p,n)e^{-\gamma_n x} \right. \\ &\quad \left. + f_{i_{11}}^{(3)}(p,n)e^{\gamma_n x} + f_{i_{12}}^{(3)}(p,n)xe^{-\gamma_p x} + f_{i_{13}}^{(3)}(p,n)xe^{\gamma_p x} \right. \\ &\quad \left. + \sum_{\substack{m=1 \\ m \neq n}}^N \left(f_{i_4}^{(3)}(p,n,m)e^{-\gamma_m x} + f_{i_5}^{(3)}(p,n,m)e^{\gamma_m x} \right) \right]. \end{aligned} \quad (32)$$

where $f_{v_{1 \sim 13}}^{(3)}$ and $f_{i_{1 \sim 13}}^{(3)}$ are the coefficients given in Appendix A depending upon whether the case is symmetrical or not.

D. Iteration 4

The diagram is the same as in Iteration 2 (shown in Fig. 3). The general subscript indices of (17) are q and p , where p is the general index of Iteration 3. Correspondingly, the virtual p.u.l. distributed voltage and current sources become

$$e_{A,q}^{(4)}(x) = - \sum_{\substack{p=1 \\ p \neq q}}^N z'_{qp} i_p^{(3)}(x), \quad q_{A,q}^{(4)}(x) = - \sum_{\substack{p=1 \\ p \neq q}}^N y'_{qp} v_p^{(3)}(x). \quad (33)$$

The elements of source vector due to Part A are given by

$$\begin{aligned} w_{1,A}^s &= e^{-\gamma_q d} \left\{ - \sum_{\substack{p=1 \\ p \neq q}}^N \left\{ B_1^{(4)+}(q,p)K_{11}^{(4)} + B_2^{(4)+}(q,p)K_{q+,p} + \right. \right. \\ &\quad \left. \left. + B_3^{(4)+}(q,p)K_{q+} + B_6^{(4)+}(q,p)K_{12}^{(4)} \right. \right. \\ &\quad \left. \left. + B_7^{(4)+}(q,p) \left(\frac{de^{\gamma_{q,p}^+ d}}{\gamma_{q,p}^+} - \frac{e^{\gamma_{q,p}^+ d} - 1}{(\gamma_{q,p}^+)^2} \right) + B_8^{(4)+}(q,p)K_{13}^{(4)} \right. \right. \\ &\quad \left. \left. + B_9^{(4)+} \left(\frac{d^2 e^{\gamma_{q,p}^+ d}}{\gamma_{q,p}^+} - \frac{2de^{\gamma_{q,p}^+ d}}{(\gamma_{q,p}^+)^2} + \frac{2e^{\gamma_{q,p}^+ d} - 2}{(\gamma_{q,p}^+)^3} \right) \right. \right. \\ &\quad \left. \left. + \sum_{\substack{n=1 \\ n \neq p}}^N \left[B_{10}^{(4)+}(q,p,n)K_{14}^{(4)} + B_{11}^{(4)+}(q,p,n)K_{q+,n} \right. \right. \right. \end{aligned}$$

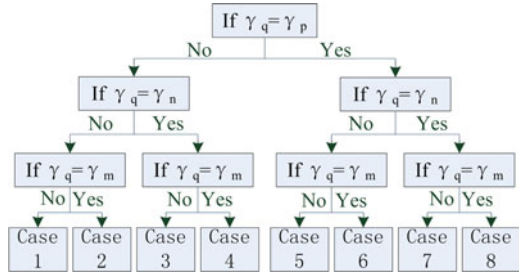


Fig. 5. Symmetry structure of Iteration 4.

$$\begin{aligned}
& + B_{12}^{(4)+}(q, p, n)K_{15}^{(4)} + B_{13}^{(4)+}(q, p, n) \\
& \times \left(\frac{de^{\gamma_{q,n}^+ d}}{\gamma_{q,n}^+} - \frac{e^{\gamma_{q,n}^+ d} - 1}{(\gamma_{q,p}^+)^2} \right) \\
& + \sum_{\substack{m=1 \\ m \neq n}}^N \left(B_4^{(4)+}(q, p, n, m)K_{16}^{(4)} \right. \\
& \quad \left. + B_5^{(4)+}(q, p, n, m)K_{q+,m-} \right) \Bigg] \Bigg\} \Bigg\} \\
\end{aligned}$$

$$\begin{aligned}
w_{2,A}^s = & \sum_{\substack{p=1 \\ p \neq q}}^N \left\{ B_1^{(4)-}(q, p)K_{q-,p-} + B_2^{(4)-}(q, p)K_{21}^{(4)} \right. \\
& + B_3^{(4)-}(q, p)K_{q-} + B_6^{(4)-}(q, p) \left(\frac{de^{-\gamma_{q,p}^+ d}}{-\gamma_{q,p}^+} - \frac{e^{-\gamma_{q,p}^+ d} - 1}{(\gamma_{q,p}^+)^2} \right) \\
& + B_7^{(4)-}(q, p)K_{22}^{(4)} + B_9^{(4)-}K_{23}^{(4)} \\
& + B_8^{(4)-}(q, p) \left(\frac{d^2 e^{-\gamma_{q,p}^+ d}}{-\gamma_{q,p}^+} - \frac{2de^{-\gamma_{q,p}^+ d}}{(\gamma_{q,p}^+)^2} + \frac{2e^{-\gamma_{q,p}^+ d} - 2}{-(\gamma_{q,p}^+)^3} \right) \\
& + \sum_{\substack{n=1 \\ n \neq p}}^N \left[B_{10}^{(4)-}(q, p, n)K_{q-,n-} + B_{11}^{(4)-}(q, p, n)K_{24}^{(4)} \right. \\
& + B_{12}^{(4)-}(q, p, n) \left(\frac{de^{-\gamma_{q,n}^+ d}}{-\gamma_{q,n}^+} - \frac{e^{-\gamma_{q,n}^+ d} - 1}{(\gamma_{q,n}^+)^2} \right) \\
& + B_{13}^{(4)-}(q, p, n)K_{25}^{(4)} + \sum_{\substack{m=1 \\ m \neq n}}^N \left(B_4^{(4)-}(q, p, n, m)K_{q-,m-} \right. \\
& \quad \left. + B_5^{(4)-}(q, p, n, m)K_{26}^{(4)} \right) \Bigg] \Bigg\}.
\end{aligned} \tag{34}$$

where $K_{11}^{(4)}$, $K_{12}^{(4)}$, $K_{13}^{(4)}$, $K_{14}^{(4)}$, $K_{15}^{(4)}$, $K_{16}^{(4)}$, and $K_{21}^{(4)}$, $K_{22}^{(4)}$, $K_{23}^{(4)}$, $K_{24}^{(4)}$, $K_{25}^{(4)}$, and $K_{26}^{(4)}$ are determined according to the correlations between the propagation constants (see Fig. 5) as follows:

Case 1 For $(\gamma_q \neq \gamma_p)$, $(\gamma_q \neq \gamma_n)$ and $(\gamma_q \neq \gamma_m)$:

$$\begin{aligned}
K_{11}^{(4)} &= K_{q+,p-}, \quad K_{21}^{(4)} = K_{p+,q-} \\
K_{12}^{(4)} &= \frac{de^{\gamma_{q,p}^- d}}{\gamma_{q,p}^-} - \frac{e^{\gamma_{q,p}^- d}}{(\gamma_{q,p}^-)^2} + \frac{1}{(\gamma_{q,p}^-)^2} \\
K_{22}^{(4)} &= \frac{de^{\gamma_{p,q}^- d}}{\gamma_{p,q}^-} - \frac{e^{\gamma_{p,q}^- d}}{(\gamma_{p,q}^-)^2} + \frac{1}{(\gamma_{p,q}^-)^2} \\
K_{13}^{(4)} &= \frac{d^2 e^{\gamma_{q,p}^- d}}{\gamma_{q,p}^-} - \frac{2de^{\gamma_{q,p}^- d}}{(\gamma_{q,p}^-)^2} + \frac{2e^{\gamma_{q,p}^- d} - 2}{(\gamma_{q,p}^-)^3} \\
K_{23}^{(4)} &= \frac{d^2 e^{\gamma_{p,q}^- d}}{\gamma_{p,q}^-} - \frac{2de^{\gamma_{p,q}^- d}}{(\gamma_{p,q}^-)^2} + \frac{2e^{\gamma_{p,q}^- d} - 2}{(\gamma_{p,q}^-)^3}. \\
K_{14}^{(4)} &= K_{q+,n-}, \quad K_{24}^{(4)} = K_{n+,q-} \\
K_{15}^{(4)} &= \frac{de^{\gamma_{q,n}^- d}}{\gamma_{q,n}^-} - \frac{e^{\gamma_{q,n}^- d} - 1}{(\gamma_{q,n}^-)^2} \\
K_{25}^{(4)} &= \frac{de^{\gamma_{n,q}^- d}}{\gamma_{n,q}^-} - \frac{e^{\gamma_{n,q}^- d} - 1}{(\gamma_{n,q}^-)^2}. \\
K_{16}^{(4)} &= K_{q+,m-}, \quad K_{26}^{(4)} = K_{m+,q-}.
\end{aligned} \tag{35}$$

Case 2 For $(\gamma_q \neq \gamma_p)$, $(\gamma_q \neq \gamma_n)$ and $(\gamma_q = \gamma_m)$:

$$\begin{aligned}
K_{11}^{(4)} &= K_{q+,p-}, \quad K_{21}^{(4)} = K_{p+,q-}, \\
K_{12}^{(4)} &= \frac{de^{\gamma_{q,p}^- d}}{\gamma_{q,p}^-} - \frac{e^{\gamma_{q,p}^- d}}{(\gamma_{q,p}^-)^2} + \frac{1}{(\gamma_{q,p}^-)^2} \\
K_{22}^{(4)} &= \frac{de^{\gamma_{p,q}^- d}}{\gamma_{p,q}^-} - \frac{e^{\gamma_{p,q}^- d}}{(\gamma_{p,q}^-)^2} + \frac{1}{(\gamma_{p,q}^-)^2} \\
K_{13}^{(4)} &= \frac{d^2 e^{\gamma_{q,p}^- d}}{\gamma_{q,p}^-} - \frac{2de^{\gamma_{q,p}^- d}}{(\gamma_{q,p}^-)^2} + \frac{2e^{\gamma_{q,p}^- d} - 2}{(\gamma_{q,p}^-)^3} \\
K_{23}^{(4)} &= \frac{d^2 e^{\gamma_{p,q}^- d}}{\gamma_{p,q}^-} - \frac{2de^{\gamma_{p,q}^- d}}{(\gamma_{p,q}^-)^2} + \frac{2e^{\gamma_{p,q}^- d} - 2}{(\gamma_{p,q}^-)^3}. \\
K_{14}^{(4)} &= K_{q+,n-}, \quad K_{24}^{(4)} = K_{n+,q-} \\
K_{15}^{(4)} &= \frac{de^{\gamma_{q,n}^- d}}{\gamma_{q,n}^-} - \frac{e^{\gamma_{q,n}^- d} - 1}{(\gamma_{q,n}^-)^2} \\
K_{25}^{(4)} &= \frac{de^{\gamma_{n,q}^- d}}{\gamma_{n,q}^-} - \frac{e^{\gamma_{n,q}^- d} - 1}{(\gamma_{n,q}^-)^2}. \\
K_{16}^{(4)} &= d, \quad K_{26}^{(4)} = d.
\end{aligned} \tag{36}$$

Case 3 For $(\gamma_q \neq \gamma_p)$, $(\gamma_q = \gamma_n)$ and $(\gamma_q \neq \gamma_m)$:

$$\begin{aligned}
K_{11}^{(4)} &= K_{q+,p-}, \quad K_{21}^{(4)} = K_{p+,q-} \\
K_{12}^{(4)} &= \frac{de^{\gamma_{q,p}^- d}}{\gamma_{q,p}^-} - \frac{e^{\gamma_{q,p}^- d}}{(\gamma_{q,p}^-)^2} + \frac{1}{(\gamma_{q,p}^-)^2} \\
K_{22}^{(4)} &= \frac{de^{\gamma_{p,q}^- d}}{\gamma_{p,q}^-} - \frac{e^{\gamma_{p,q}^- d}}{(\gamma_{p,q}^-)^2} + \frac{1}{(\gamma_{p,q}^-)^2}
\end{aligned}$$

$$\begin{aligned}
K_{13}^{(4)} &= \frac{d^2 e^{\gamma_{q,p}^- d}}{\gamma_{q,p}^-} - \frac{2 d e^{\gamma_{q,p}^- d}}{(\gamma_{q,p}^-)^2} + \frac{2 e^{\gamma_{q,p}^- d} - 2}{(\gamma_{q,p}^-)^3} \\
K_{23}^{(4)} &= \frac{d^2 e^{\gamma_{p,q}^- d}}{\gamma_{p,q}^-} - \frac{2 d e^{\gamma_{p,q}^- d}}{(\gamma_{p,q}^-)^2} + \frac{2 e^{\gamma_{p,q}^- d} - 2}{(\gamma_{p,q}^-)^3} \\
K_{14}^{(4)} &= d, K_{24}^{(4)} = d, K_{15}^{(4)} = d^2/2 \\
K_{25}^{(4)} &= d^2/2, K_{16}^{(4)} = K_{q+,m-}, K_{26}^{(4)} = K_{m+,q-}. \quad (37)
\end{aligned}$$

Case 4 For $(\gamma_q \neq \gamma_p), (\gamma_q = \gamma_n)$ and $(\gamma_q = \gamma_m)$:

$$\begin{aligned}
K_{11}^{(4)} &= K_{q+,p-}, \quad K_{21}^{(4)} = K_{p+,q-} \\
K_{12}^{(4)} &= \frac{d e^{\gamma_{q,p}^- d}}{\gamma_{q,p}^-} - \frac{e^{\gamma_{q,p}^- d}}{(\gamma_{q,p}^-)^2} + \frac{1}{(\gamma_{q,p}^-)^2} \\
K_{22}^{(4)} &= \frac{d e^{\gamma_{p,q}^- d}}{\gamma_{p,q}^-} - \frac{e^{\gamma_{p,q}^- d}}{(\gamma_{p,q}^-)^2} + \frac{1}{(\gamma_{p,q}^-)^2} \\
K_{13}^{(4)} &= \frac{d^2 e^{\gamma_{q,p}^- d}}{\gamma_{q,p}^-} - \frac{2 d e^{\gamma_{q,p}^- d}}{(\gamma_{q,p}^-)^2} + \frac{2 e^{\gamma_{q,p}^- d} - 2}{(\gamma_{q,p}^-)^3} \\
K_{23}^{(4)} &= \frac{d^2 e^{\gamma_{p,q}^- d}}{\gamma_{p,q}^-} - \frac{2 d e^{\gamma_{p,q}^- d}}{(\gamma_{p,q}^-)^2} + \frac{2 e^{\gamma_{p,q}^- d} - 2}{(\gamma_{p,q}^-)^3} \\
K_{14}^{(4)} &= d, K_{24}^{(4)} = d, K_{15}^{(4)} = d^2/2 \\
K_{25}^{(4)} &= d^2/2, K_{16}^{(4)} = d, K_{26}^{(4)} = d. \quad (38)
\end{aligned}$$

Case 5 For $(\gamma_q = \gamma_p), (\gamma_q \neq \gamma_n)$ and $(\gamma_q \neq \gamma_m)$:

$$\begin{aligned}
K_{11}^{(4)} &= d, K_{21}^{(4)} = d, K_{12}^{(4)} = d^2/2 \\
K_{22}^{(4)} &= d^2/2, K_{13}^{(4)} = d^3/3, K_{23}^{(4)} = d^3/3 \\
K_{14}^{(4)} &= K_{q+,n-}, \quad K_{24}^{(4)} = K_{n+,q-} \\
K_{15}^{(4)} &= \frac{d e^{\gamma_{q,n}^- d}}{\gamma_{q,n}^-} - \frac{e^{\gamma_{q,n}^- d} - 1}{(\gamma_{q,n}^-)^2} \\
K_{25}^{(4)} &= \frac{d e^{\gamma_{n,q}^- d}}{\gamma_{n,q}^-} - \frac{e^{\gamma_{n,q}^- d} - 1}{(\gamma_{n,q}^-)^2} \\
K_{16}^{(4)} &= K_{q+,m-}, \quad K_{26}^{(4)} = K_{m+,q-}. \quad (39)
\end{aligned}$$

Case 6 For $(\gamma_q = \gamma_p), (\gamma_q \neq \gamma_n)$ and $(\gamma_q = \gamma_m)$:

$$\begin{aligned}
K_{11}^{(4)} &= d, K_{21}^{(4)} = d, K_{12}^{(4)} = d^2/2 \\
K_{22}^{(4)} &= d^2/2, K_{13}^{(4)} = d^3/3, K_{23}^{(4)} = d^3/3 \\
K_{14}^{(4)} &= K_{q+,n-}, \quad K_{24}^{(4)} = K_{n+,q-} \\
K_{15}^{(4)} &= \frac{d e^{\gamma_{q,n}^- d}}{\gamma_{q,n}^-} - \frac{e^{\gamma_{q,n}^- d} - 1}{(\gamma_{q,n}^-)^2} \\
K_{25}^{(4)} &= \frac{d e^{\gamma_{n,q}^- d}}{\gamma_{n,q}^-} - \frac{e^{\gamma_{n,q}^- d} - 1}{(\gamma_{n,q}^-)^2} \\
K_{16}^{(4)} &= d, \quad K_{26}^{(4)} = d. \quad (40)
\end{aligned}$$

Case 7 For $(\gamma_q = \gamma_p), (\gamma_q = \gamma_n)$ and $(\gamma_q \neq \gamma_m)$:

$$\begin{aligned}
K_{11}^{(4)} &= d, K_{21}^{(4)} = d, K_{12}^{(4)} = d^2/2 \\
K_{22}^{(4)} &= d^2/2, K_{13}^{(4)} = d^3/3, K_{23}^{(4)} = d^3/3 \\
K_{14}^{(4)} &= d, K_{24}^{(4)} = d, K_{15}^{(4)} = d^2/2 \\
K_{25}^{(4)} &= d^2/2. K_{16}^{(4)} = K_{q+,m-}, K_{26}^{(4)} = K_{m+,q-}. \quad (41)
\end{aligned}$$

Case 8 For $(\gamma_q = \gamma_p), (\gamma_q = \gamma_n)$ and $(\gamma_q = \gamma_m)$:

$$\begin{aligned}
K_{11}^{(4)} &= d, K_{21}^{(4)} = d, K_{12}^{(4)} = d^2/2 \\
K_{22}^{(4)} &= d^2/2, K_{13}^{(4)} = d^3/3, K_{23}^{(4)} = d^3/3 \\
K_{14}^{(4)} &= d, K_{24}^{(4)} = d, K_{15}^{(4)} = d^2/2 \\
K_{25}^{(4)} &= d^2/2, K_{16}^{(4)} = d, K_{26}^{(4)} = d. \quad (42)
\end{aligned}$$

The elements of source vector due to part B keep the same form as in (13) except for the index.

E. More Iterations

Paul has shown in [3] (equivalent to only one iteration) the accuracy is acceptable for crosstalk prediction if the WCA is satisfied. Generally speaking, the accuracies after Iteration 4 for most cases will suffice since the values of typical coupling factors are between 0.05 and 0.2 [8], [16], [17]. This conclusion was further validated using crosstalk prediction examples by the rigorous conceptual and theoretical explanation of the convergence speed in [10] and [11]. The validation results presented later will show the relation of the accuracy and the number of iterations.

V. VALIDATION OF THE PROPOSED ALGORITHM

In order to demonstrate the validity of the proposed DARIT-field algorithm for the calculation of EMP coupling to MTLs, we present five case studies which are commonly encountered. Except for Example 2, all the MTLs were illuminated by the incoming EMP wave which was defined by IEC 61000-2-9 [12].

$$E(t) = E_0 k (e^{-\alpha t} - e^{-\beta t}) \quad (43)$$

where $E_0 = 5e4$, $k = 1.3$, $\alpha = 4e7$, and $\beta = 6e8$.

For each case example, the load responses are computed by the proposed DARIT-field method and the conventional stamp method (see [1], [2], and [7]) and the comparisons were made to show the agreement between these two methods.

A. Example 1: Symmetry

We consider the cases of symmetrical and unsymmetrical coupled lines as different cases because the formulae pertaining to them do not have the same form.

1) Symmetrical Coupled Lines: A symmetrical, nine-conductor microstrip structure, with length of 1cm, height of 1mm, diameter of 0.1 mm and distance between lines of 1.5 mm, over the lossy ground is considered. The relative dielectric constant and electrical conductivity of ground is 10 and 0.01 S/m,

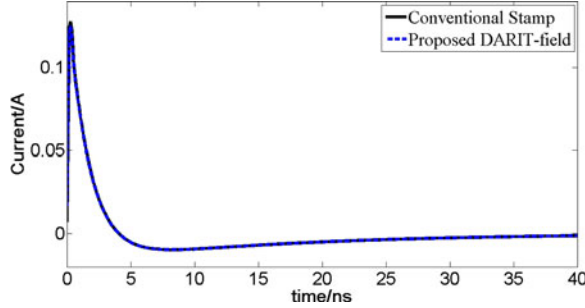


Fig. 6. Induced current waveform at far-end of line #1. (Example 1: symmetrical lines.)

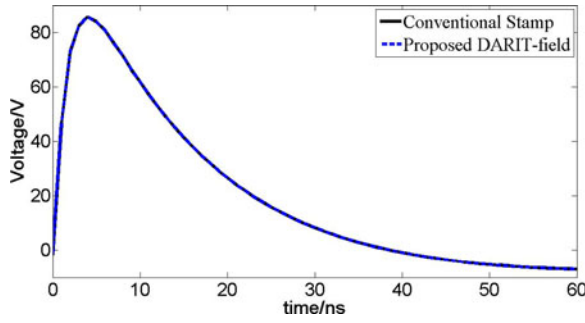


Fig. 7. Induced voltage waveform at far-end of line #1. (Example 1: unsymmetrical lines.)

respectively. The loads are 50Ω at near-end and 1 pF at far-end. $\alpha = 0^\circ$, $\psi = 30^\circ$, and $\phi = 0^\circ$ (the definitions of these angles are given in [2]) for the incoming EMP wave. Fig. 6 shows a sample of the computed waveforms (after Iteration 4 described in Section IV) compared to the computed waveforms from the conventional stamp method. As seen from the plots, the results are in very good agreement.

2) *Unsymmetrical Coupled Lines*: An unsymmetrical, three-conductor microstrip structure with length of 1 cm and height of 1 mm is considered. The loads on both sides are terminated with pseudomatching resistors (it's required to completely match a MTLs with a load network wherein there are not only loads between each line and the reference conductor but also between each line. In this example, it is not so strictly matched). $R_1 = 86.84 \Omega$, $R_2 = 125.46 \Omega$, and $R_3 = 104.39 \Omega$. The p.u.l. parameters of \mathbf{R}' , \mathbf{L}' , \mathbf{G}' , and \mathbf{C}' were given in Fig. 6 of [18]. The incoming EMP is the same as in the aforementioned example. The results after Iteration 4 depicted in Fig. 7 are in good agreement with the results from the conventional stamp method.

B. Example 2: Coupling Factors (CF)

The purpose of this example is to quantitatively illustrate the accuracy of the proposed method as a function of different coupling factors. The coupling factor is defined by the p.u.l. inductance parameters as follows:

$$\text{CF} = \max_{\substack{i, j \\ i \neq j}} \sqrt{l'_{ij}^2 / (l'_{ii} l'_{jj})} \quad (44)$$

where l'_{ij} is the (i, j) th cell of the \mathbf{L}' matrix.

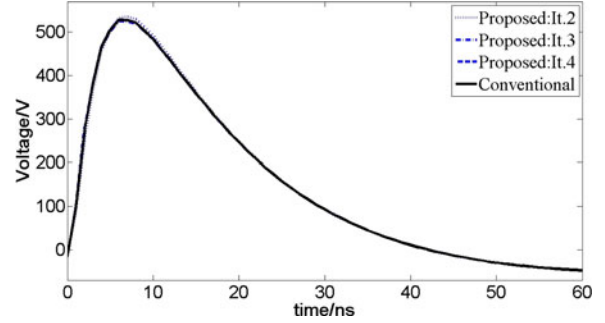


Fig. 8. Far-end response of line #1 with coupling factors of 0.05 (Example 2: coupling factors.)

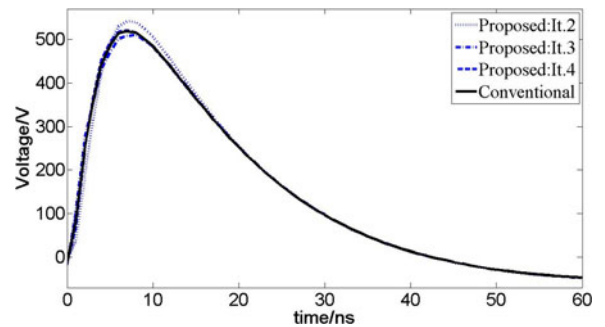


Fig. 9. Far-end response of line #1 with coupling factors of 0.25 (Example 2: Coupling factors).

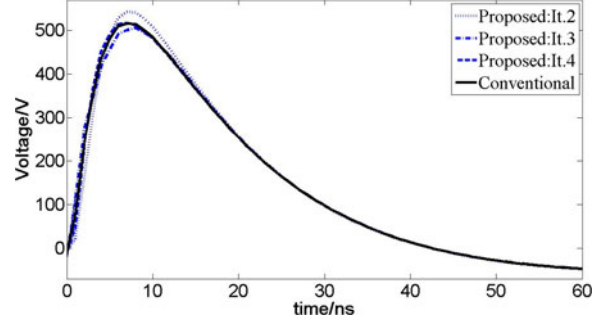


Fig. 10. Far-end response of line #1 with coupling factors of 0.35. (Example 2: Coupling factors).

A symmetrical and lossy three-conductor microstrip structure with the length, height, and diameter equal to 7.5 cm, 2 mm, and 0.2 mm, respectively, which above the lossy ground is considered. The relative dielectric constant and electrical conductivity of ground is 10 and 0.01 S/m , respectively. The loads on both sides are 50Ω . We produce three cases with coupling factors of 0.05, 0.25, and 0.35 by changing the distance between lines to 6.76 mm, 2.14 mm, and 1.50 mm, respectively. The wave form of exciting source is the IEC HEMP pulse with $\alpha = 0^\circ$, $\psi = 30^\circ$, and $\phi = 0^\circ$. Figs. 8–10 show the time response of line #1 with the varied coupling factors. We can see that the proposed DARIT-field approach agrees well with the conventional stamp method with the coupling factors of 0.05 only after Iteration 2. Then, we increase the value to 0.25, it would take 3 iterations to get the satisfactory agreement. When the CF is 0.35 for

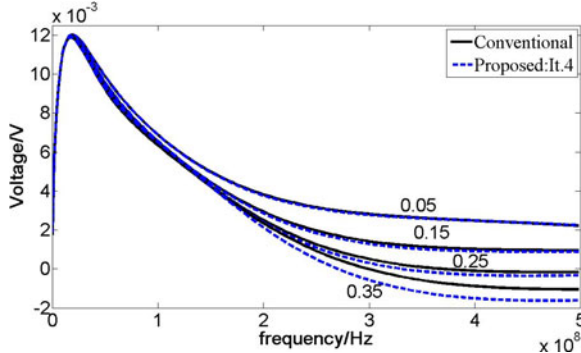


Fig. 11. Far-end response of line #1 in the frequency domain with different coupling factors. (Example 2: Coupling factors).

TABLE I
RELATIVE ERRORS CORRESPONDING TO ITERATION 1, 2, 3, AND 4 (EXAMPLE 2)

CF	$\epsilon/time(s)$	$\epsilon/time(s)$	$\epsilon/time(s)$	$\epsilon/time(s)$
	iteration 1	iteration 2	iteration 3	iteration 4
0.05	1.33e-2/0.24	6.10e-4/0.65	4.88e-4/1.11	2.94e-4/3.13
0.15	3.40e-2/0.21	2.12e-3/0.57	1.29e-3/1.04	1.10e-3/3.15
0.25	1.51e-1/0.21	1.92e-2/0.56	3.30e-3/1.04	1.98e-3/3.12
0.35	2.43e-1/0.20	4.31e-2/0.56	1.00e-2/1.04	9.25e-3/3.12

the same length of line, only after Iteration 4 the solutions are satisfactory.

Fig. 11 shows the frequency response of line #1 with the coupling factors varied in the range of 0.05–0.35. The interconnects are excited by the continuous electromagnetic wave of amplitude equals to 1 V/m and the frequency range of the source is up to 500 MHz. Note that in the higher frequency range there are slight differences between the proposed method and the conventional stamp method.

In order to quantify the differences, a relative error ϵ based on energy norm in frequency domain is defined as follows:

$$\epsilon \cong \left| \frac{\sum_{k=1}^{N_f} |S_1(f_k)|^2 - \sum_{k=1}^{N_f} |S_2(f_k)|^2}{\sum_{k=1}^{N_f} |S_1(f_k)|^2} \right| \quad (45)$$

where N_f is the number of sampling points in the frequency domain and f_k is the value of frequency at the k th sampling point. S_1 and S_2 represent the reference value obtained by the conventional stamp method and the value obtained by the proposed method, respectively.

The relative errors ϵ together with the time cost for 10^3 frequency points (runs on PC with Intel Core i3 2.8 GHz CPU, 2 G RAM) after Iteration 3 and 4 are presented in Table I, respectively. The results are satisfactory since the relative errors ϵ defined in (45) are quite small, only around 0.93% for the case of CF = 0.35 after Iteration 4. Obviously, one can make a choice between accuracy and efficiency as needed.

It is worthwhile to point out that there are some sensible parameters, e.g., the coupling factor and the ratio of the length of the line to the minimum wavelength of interest of the exiting EMP wave, which may affect the convergence speed and the accuracy. The theoretical analysis of these predictions are described in [11]. In some special cases with a large value of coupling factor and length of line, another iteration or even more

TABLE II
TEST CASES OF TERMINAL LOADS VARIED AT FAR END (EXAMPLE 3)

Cases	Types	Values
1	R_L	1 Ω
2	L	10 nH
3	C	1 pF
4	R_L, L, C in series	50 Ω , 1 nH, 1 pF

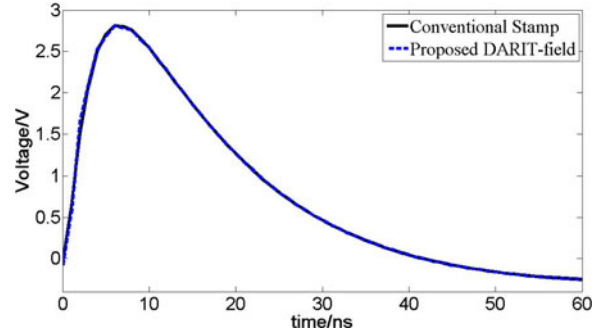


Fig. 12. Far-end response of line #1 for case 1. (Example 3: Loads).

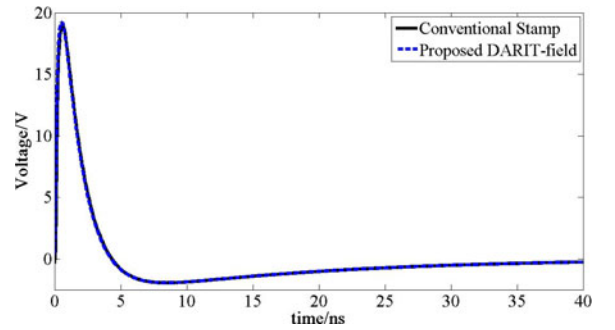


Fig. 13. Far-end response of line #1 for case 2. (Example 3: loads.)

iterations could be done following the same procedure in order to get more accurate solutions.

C. Example 3: Loads

Since the reflection coefficients in the solutions are different from the line parameters as they depend on both the line properties and the nature of the termination impedance, the objective of this example is to illustrate the applicability of the DARIT-field method to cases terminated with different loads. The MTLs are similar to the one shown in Fig. 6 with the exception that the values of the loads at the far end are varied. Several typical test cases of terminal loads are shown in Table II. The results of Case 3 for capacitive load are already shown in Fig. 6. Figs. 12–14 and Fig. 6 (Case 4) show the results from the proposed method (after Iteration 4) and the conventional stamp method, indicating good agreement.

D. Example 4: Computational Speed

This example illustrates the computational complexity of the proposed method as a function of the number of lines. The comparison between the DARIT-field and the conventional stamp method makes sense since the sampling points (10^3) remains the same. The microstrip structure consisting of different numbers

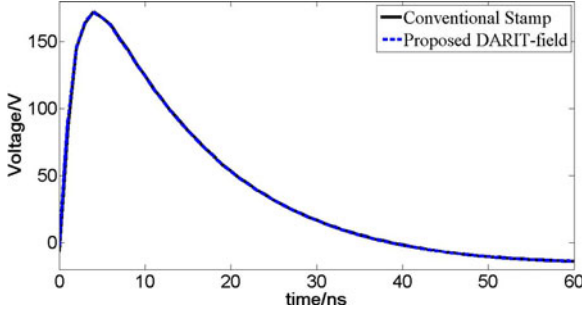


Fig. 14. Far-end response of line #1 for case 4. (Example 3: loads.)

TABLE III
CPU COST COMPARISON (EXAMPLE 4)

Num. of Lines (N)	Conventional Stamp	Proposed DARIT	
	Time Cost (s)	Iteration 3 (s)	Iteration 4 (s)
9	1795.34	4.20	38.59
15	3092.74	20.50	127.34
24	4672.33	41.38	485.43
30	5831.93	78.24	890.62
36	7581.00	134.83	1452.67
45	8977.75	270.79	2965.12

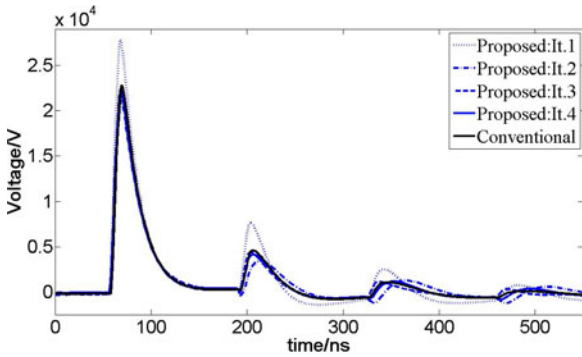


Fig. 15. Induced voltage waveform of far-end of line #1. (Example 5: Aerial Lines Example.)

of conductors with length of 1 cm, height of 1 mm, diameter of 0.1 mm, and distance between lines of 1 mm above the lossy ground is considered. We produce six cases with the number of lines equal to 9, 15, 24, 30, 36, 45, respectively. Table III shows several cases with varied numbers of lines. As can be seen, the proposed approach has much less CPU cost compared to the conventional method.

E. Example 5: Aerial Lines Example

This example demonstrates the validity to handle EMP coupling to aerial MTLs. A symmetrical three-conductor structure over the lossy ground is considered, with length of 20 m, height of 1 m, diameter of 1 mm, and distance between lines of 2 m. The both loads are 50Ω . The relative dielectric constant and electrical conductivity of ground is 10 and 0.01 S/m, respectively. $\alpha = 0^\circ$, $\psi = 30^\circ$, and $\phi = 0^\circ$ for the incoming EMP wave. As seen from the plots in Fig. 15, the results after Iteration 4 agree well with the conventional stamp method.

VI. SUMMARY AND CONCLUSION

The proposed DARIT-field method has been developed and validated over a wide range of cases including symmetry, coupling factors, loads, computational speed, aerial lines, etc. The proposed method provides an iterative approach to predict EMP coupling to MTLs. At each iteration, each line is excited by the existing sources which are the general terms due to the incoming EMP and the virtual voltage and current sources on the adjacent lines obtained at the previous iteration. The solutions and the equivalent virtual exciting sources at each iteration could be updated in an analytical representation in terms of the combined voltage wave, so that the fast convergence and computational efficiency can be achieved to show its definite advantages over the other methods. The method also has the convenience of illustrating the factors affecting the coupling, the capability to handle MTLs with different types of loads, and a large number of lines efficiently. In addition, the proposed method is flexible, allowing the user to make a compromise between computational cost and accuracy by selecting the number of iterations.

For the situations with larger coupling factors and less lossy terminations, the method has limitations due to the need of more iterations to get the required accuracy or it might even become unstable when the condition of convergence cannot be satisfied. The dependence of coupling factor, the terminations and other factors on the convergence and on the accuracy of the method needs further studies, which are underway.

Future work will also involve the transform of the proposed method from the frequency domain to the time domain in order to handle the cases with nonlinear and time-varying loads.

APPENDIX A

A. Coefficients of f_v and f_i

We use the Taylor model and take into account the reflection effects of earth for the incoming EMP wave. For the i th conductor of MTLs, the equations could be expressed by

$$\begin{aligned} V'_{s,i}(x) &= -j\omega\mu_0 \int_0^h H_y^e(x, 0, z) dz + E_x^e(x, 0, 0) \\ I'_{s,i}(x) &= -j\omega \sum_{k=1}^N c'_{ik} \int_0^h E_z^e(x, 0, z) dz \end{aligned} \quad (46)$$

where c'_{ik} is the element of the capacitance matrix, and $H_y^e(x, 0, z)$, $E_x^e(x, 0, 0)$, and $E_z^e(x, 0, z)$ are the total fields with the absence of transmission line (more details of the expressions see [2])

The exciting sources for line i are given by

$$V'_{s,i}(x) = f_v e^{-jkx \cos \psi \cos \phi}, \quad I'_{s,i}(x) = f_i e^{-jkx \cos \psi \cos \phi} \quad (47)$$

where the coefficients of f_v and f_i are given as follows:

$$\begin{aligned} f_v &= \frac{c\mu_0 E_0}{z_0} \left\{ \sin \alpha \sin \phi [1 - (1 - R_h)e^{-jkh \sin \psi} \right. \\ &\quad \left. - R_h e^{-2jkh \sin \psi}] + \frac{\cos \alpha \cos \phi}{\sin \psi} [1 - (1 - R_v)e^{-jkh \sin \psi} \right. \\ &\quad \left. - R_v e^{-2jkh \sin \psi}] \right\} \end{aligned}$$

$$\begin{aligned}
& -R_v e^{-2jkh \sin \psi} \Big] \Big\} + E_0 [\cos \alpha \sin \psi \cos \phi (1 - R_v) \\
& + \sin \alpha \sin \phi (1 + R_h)] e^{-jkh \sin \psi} \\
f_i &= \frac{cE_0 \cos \alpha \cos \psi}{\sin \psi} \left\{ \sum_{k=1}^N c'_{ik} [(1 - R_v) e^{-jkh \sin \psi} \right. \\
& \left. + R_v e^{-2jkh \sin \psi} - 1] \right\}. \tag{48}
\end{aligned}$$

where R_v and R_h are the vertical and horizontal Fresnel reflection coefficients, respectively. For the definitions of α , ψ , and ϕ [2].

B. Coefficients of $f_{v_{1 \sim 7}}^{(2)}$ and $f_{i_{1 \sim 7}}^{(2)}$

1) Unsymmetrical Cases of MTLs ($\gamma_n \neq \gamma_m$):

$$\begin{aligned}
f_{v_1}^{(2)}(n) &= \frac{1}{2} \left[\left(w_n^{(2)}(0) \right)_+ - \frac{f_v(n) + Z_{c,n} f_i(n)}{\gamma_n - jk \cos \psi \cos \phi} \right. \\
&+ \sum_{\substack{m=1 \\ m \neq n}}^N \left(\frac{B_1^{(2)+}(n, m)}{\gamma_{n,m}^-} + \frac{B_2^{(2)+}(n, m)}{\gamma_{n,m}^+} \right. \\
&\quad \left. \left. + \frac{B_3^{(2)+}(n, m)}{\gamma_n - jk \cos \psi \cos \phi} \right) \right] \\
f_{v_2}^{(2)}(n) &= \frac{1}{2} \left[\left(w_n^{(2)}(d) \right)_- e^{-\gamma_n d} \right. \\
&+ \frac{f_v(n) - Z_{c,n} f_i(n)}{\gamma_n + jk \cos \psi \cos \phi} e^{-(\gamma_n + jk \cos \psi \cos \phi)d} \\
&+ \sum_{\substack{m=1 \\ m \neq n}}^N \left(B_1^{(2)-}(n, m) K_{n-, m-} + B_2^{(2)-}(n, m) K_{m+, n-} \right. \\
&\quad \left. \left. + B_3^{(2)-}(n, m) K_{n-} \right) \right] \\
f_{v_3}^{(2)}(n) &= \frac{1}{2} \left[\frac{f_v(n) + Z_{c,n} f_i(n)}{\gamma_n - jk \cos \psi \cos \phi} - \frac{f_v(n) - Z_{c,n} f_i(n)}{\gamma_n + jk \cos \psi \cos \phi} \right. \\
&- \sum_{\substack{m=1 \\ m \neq n}}^N \left(\frac{B_3^{(2)+}(n, m)}{\gamma_n - jk \cos \psi \cos \phi} - \frac{B_3^{(2)-}(n, m)}{\gamma_n + jk \cos \psi \cos \phi} \right) \\
f_{v_4}^{(2)}(n, m) &= -\frac{1}{2} \left(\frac{B_1^{(2)+}(n, m)}{\gamma_{n,m}^-} - \frac{B_1^{(2)-}(n, m)}{\gamma_{n,m}^+} \right) \\
f_{v_5}^{(2)}(n, m) &= -\frac{1}{2} \left(\frac{B_2^{(2)+}(n, m)}{\gamma_{n,m}^+} + \frac{B_2^{(2)-}(n, m)}{\gamma_{n,m}^-} \right) \\
f_{v_6}^{(2)}(n) &= 0, \quad f_{v_7}^{(2)}(n) = 0. \\
f_{i_1}^{(2)}(n) &= \frac{f_{v_1}^{(2)}(n)}{Z_{c,n}}, \quad f_{i_2}^{(2)}(n) = -\frac{f_{v_2}^{(2)}(n)}{Z_{c,n}} \tag{49}
\end{aligned}$$

$$\begin{aligned}
f_{i_3}^{(2)}(n) &= \frac{0.5}{Z_{c,n}} \left[\frac{f_v(n) + Z_{c,n} f_i(n)}{\gamma_n - jk \cos \psi \cos \phi} + \frac{f_v(n) - Z_{c,n} f_i(n)}{\gamma_n + jk \cos \psi \cos \phi} \right. \\
&- \sum_{\substack{m=1 \\ m \neq n}}^N \left(\frac{B_3^{(2)+}(n, m)}{\gamma_n - jk \cos \psi \cos \phi} + \frac{B_3^{(2)-}(n, m)}{\gamma_n + jk \cos \psi \cos \phi} \right) \\
f_{i_4}^{(2)}(n, m) &= -\frac{0.5}{Z_{c,n}} \left(\frac{B_1^{(2)+}(n, m)}{\gamma_{n,m}^-} + \frac{B_1^{(2)-}(n, m)}{\gamma_{n,m}^+} \right) \\
f_{i_5}^{(2)}(n, m) &= -\frac{0.5}{Z_{c,n}} \left(\frac{B_2^{(2)+}(n, m)}{\gamma_{n,m}^+} + \frac{B_2^{(2)-}(n, m)}{\gamma_{n,m}^-} \right) \\
f_{i_6}^{(2)}(n) &= 0, \quad f_{i_7}^{(2)}(n) = 0. \tag{50}
\end{aligned}$$

2) Symmetrical Cases of MTLs ($\gamma_n = \gamma_m$):

$$\begin{aligned}
f_{v_1}^{(2)}(n) &= \frac{1}{2} \left[\left(w_n^{(2)}(0) \right)_+ - \frac{f_v(n) + Z_{c,n} f_i(n)}{\gamma_n - jk \cos \psi \cos \phi} \right. \\
&+ \sum_{\substack{m=1 \\ m \neq n}}^N \left(\frac{B_2^{(2)+}(n, m)}{\gamma_{n,m}^+} \right. \\
&\quad \left. \left. + \frac{B_3^{(2)+}(n, m)}{\gamma_n - jk \cos \psi \cos \phi} \right) \right] \\
f_{v_2}^{(2)}(n) &= \frac{1}{2} \left[\left(w_n^{(2)}(d) \right)_- e^{-\gamma_n d} \right. \\
&+ \frac{f_v(n) - Z_{c,n} f_i(n)}{\gamma_n + jk \cos \psi \cos \phi} e^{-(\gamma_n + jk \cos \psi \cos \phi)d} \\
&+ \sum_{\substack{m=1 \\ m \neq n}}^N \left(B_1^{(2)-}(n, m) K_{n-, m-} \right. \\
&\quad \left. \left. + B_2^{(2)-}(n, m) d + B_3^{(2)-}(n, m) K_{n-} \right) \right] \\
f_{v_3}^{(2)}(n) &= \frac{1}{2} \left[\frac{f_v(n) + Z_{c,n} f_i(n)}{\gamma_n - jk \cos \psi \cos \phi} - \frac{f_v(n) - Z_{c,n} f_i(n)}{\gamma_n + jk \cos \psi \cos \phi} \right. \\
&- \sum_{\substack{m=1 \\ m \neq n}}^N \left(\frac{B_3^{(2)+}(n, m)}{\gamma_n - jk \cos \psi \cos \phi} \right. \\
&\quad \left. \left. - \frac{B_3^{(2)-}(n, m)}{\gamma_n + jk \cos \psi \cos \phi} \right) \right] \\
f_{v_4}^{(2)}(n, m) &= \frac{B_1^{(2)-}(n, m)}{\gamma_{n,m}^+}, \quad f_{v_5}^{(2)}(n, m) = -\frac{1}{2} \frac{B_2^{(2)+}(n, m)}{\gamma_{n,m}^+} \\
f_{v_6}^{(2)}(n) &= -\frac{1}{2} \sum_{\substack{m=1 \\ m \neq n}}^N B_1^{(2)+}(n, m)
\end{aligned}$$

$$\begin{aligned}
f_{v_7}^{(2)}(n) &= -\frac{1}{2} \sum_{\substack{m=1 \\ m \neq n}}^N B_2^{(2)-}(n, m) \\
f_{i_1}^{(2)}(n) &= \frac{f_{v_1}^{(2)}(n)}{Z_{c,n}}, \quad f_{i_2}^{(2)}(n) = -\frac{f_{v_2}^{(2)}(n)}{Z_{c,n}} \\
f_{i_3}^{(2)}(n) &= \frac{1}{2Z_{c,n}} \left[\frac{f_v(n) + Z_{c,p} f_i(n)}{\gamma_n - jk \cos \psi \cos \phi} + \frac{f_v(n) - Z_{c,n} f_i(n)}{\gamma_n + jk \cos \psi \cos \phi} \right. \\
&\quad \left. - \sum_{\substack{m=1 \\ m \neq n}}^N \left(\frac{B_3^{(2)+}(n, m)}{\gamma_n - jk \cos \psi \cos \phi} \right. \right. \\
&\quad \left. \left. + \frac{B_3^{(2)+}(n, m)}{\gamma_n + jk \cos \psi \cos \phi} \right) \right] \\
f_{i_4}^{(2)}(n, m) &= -\frac{B_1^{(2)-}(n, m)}{2Z_{c,n} \gamma_{n,m}^+}, \quad f_{i_5}^{(2)}(n, m) = -\frac{B_2^{(2)+}(n, m)}{2Z_{c,n} \gamma_{n,m}^+} \\
f_{i_6}^{(2)}(n) &= -\frac{0.5}{Z_{c,n}} \sum_{\substack{m=1 \\ m \neq n}}^N B_1^{(2)+}(n, m) \tag{51} \\
f_{i_7}^{(2)}(n) &= \frac{0.5}{Z_{c,n}} \sum_{\substack{m=1 \\ m \neq n}}^N B_2^{(2)-}(n, m) \tag{52}
\end{aligned}$$

C. Coefficients of $f_{v_{1 \sim 13}}^{(3)}$ and $f_{i_{1 \sim 13}}^{(3)}$

Whatever the MTLs structure is symmetrical or not, the coefficients are given as follows:

$$\begin{aligned}
f_{v_3}^{(3)}(p) &= \frac{1}{2} \left[\frac{f_v(p) + Z_{c,p} f_i(p)}{\gamma_p - jk \cos \psi \cos \phi} - \frac{f_v(p) - Z_{c,p} f_i(p)}{\gamma_p + jk \cos \psi \cos \phi} \right. \\
&\quad \left. - \sum_{\substack{n=1 \\ n \neq p}}^N \left(\frac{B_3^{(3)+}(p, n)}{\gamma_p - jk \cos \psi \cos \phi} - \frac{B_3^{(3)-}(p, n)}{\gamma_p + jk \cos \psi \cos \phi} \right) \right] \\
f_{i_3}^{(3)}(p) &= \frac{1}{2Z_{c,p}} \left[\frac{f_v(p) + Z_{c,p} f_i(p)}{\gamma_p - jk \cos \psi \cos \phi} + \frac{f_v(p) - Z_{c,p} f_i(p)}{\gamma_p + jk \cos \psi \cos \phi} \right. \\
&\quad \left. - \sum_{\substack{n=1 \\ n \neq p}}^N \left(\frac{B_3^{(3)+}(p, n)}{\gamma_p - jk \cos \psi \cos \phi} + \frac{B_3^{(3)+}(p, n)}{\gamma_p + jk \cos \psi \cos \phi} \right) \right]. \tag{53}
\end{aligned}$$

The other coefficients are determined depending upon the symmetry of the MTLs, which are given as follows.

1) If $(\gamma_p \neq \gamma_n)$ and $(\gamma_p \neq \gamma_m)$:

$$\begin{aligned}
f_{v_1}^{(3)}(p) &= \frac{1}{2} \left\{ (w_p^{(3)}(0))_+ - \frac{f_v(p) + Z_{c,p} f_i(p)}{\gamma_p - jk \cos \psi \cos \phi} \right. \\
&\quad \left. + \sum_{\substack{n=1 \\ n \neq p}}^N \left[\frac{B_1^{(3)+}(p, n)}{\gamma_{p,n}^-} + \frac{B_2^{(3)+}(p, n)}{\gamma_{p,n}^+} + \frac{B_3^{(3)+}(p, n)}{\gamma_p - jk \cos \psi \cos \phi} \right. \right. \\
&\quad \left. \left. + \frac{B_4^{(3)+}(p, n)}{\gamma_{p,n}^-} + \frac{B_5^{(3)+}(p, n)}{\gamma_{p,n}^+} \right] \right\}
\end{aligned}$$

$$\begin{aligned}
&+ \sum_{\substack{m=1 \\ m \neq n}}^N \left(\frac{B_4^{(3)+}(p, n, m)}{\gamma_{p,m}^-} + \frac{B_5^{(3)+}(p, n, m)}{\gamma_{p,m}^+} \right) \right\} \\
f_{v_2}^{(3)}(p) &= \frac{1}{2} \left\{ (w_p^{(3)}(d))_- e^{-\gamma_p d} \right. \\
&\quad \left. + \frac{f_v(p) - Z_{c,p} f_i(p)}{\gamma_p + jk \cos \psi \cos \phi} e^{-(\gamma_p + jk \cos \psi \cos \phi)d} \right. \\
&\quad \left. + \sum_{\substack{n=1 \\ n \neq p}}^N \left[B_3^{(3)-}(p, n) K_{p-} \right. \right. \\
&\quad \left. \left. + B_1^{(3)-}(p, n) K_{p-,n-} + B_2^{(3)-}(p, n) K_{n+,p-} \right. \right. \\
&\quad \left. \left. + \sum_{\substack{m=1 \\ m \neq n}}^N \left(B_4^{(3)-}(p, n, m) K_{p-,m-} - B_5^{(3)-}(p, n, m) K_{m+,p-} \right) \right] \right\} \\
f_{v_4}^{(3)}(p, n, m) &= -\frac{1}{2} \left(\frac{B_4^{(3)+}(p, n, m)}{\gamma_{m,p}^-} - \frac{B_4^{(3)-}(p, n, m)}{\gamma_{m,p}^+} \right) \\
f_{v_5}^{(3)}(p, n, m) &= -\frac{1}{2} \left(\frac{B_5^{(3)+}(p, n, m)}{\gamma_{p,m}^+} + \frac{B_5^{(3)-}(p, n, m)}{\gamma_{p,m}^-} \right) \\
f_{v_{10}}^{(3)}(p, n) &= -\frac{1}{2} \left(\frac{B_1^{(3+}(p, n)}{\gamma_{p,n}^-} - \frac{B_1^{(3-}(p, n)}{\gamma_{p,n}^+} \right) \\
f_{v_{11}}^{(3)}(p, n) &= -\frac{1}{2} \left(\frac{B_2^{(3+}(p, n)}{\gamma_{p,n}^+} + \frac{B_2^{(3-}(p, n)}{\gamma_{n,p}^-} \right) \\
f_{v_{6 \sim 9}}^{(3)}(p) &= 0, \quad f_{v_{12 \sim 13}}^{(3)}(p, n) = 0 \\
f_{i_1}^{(3)}(p) &= \frac{f_{v_1}^{(3)}(p)}{Z_{c,p}}, \quad f_{i_2}^{(3)}(p) = -\frac{f_{v_2}^{(3)}(n)}{Z_{c,p}} \tag{54} \\
f_{i_4}^{(3)}(p, n, m) &= -\frac{1}{2Z_{c,p}} \left(\frac{B_4^{(3)+}(p, n, m)}{\gamma_{p,m}^-} + \frac{B_4^{(3)-}(p, n, m)}{\gamma_{p,m}^+} \right) \\
f_{i_5}^{(3)}(p, n, m) &= -\frac{1}{2Z_{c,p}} \left(\frac{B_5^{(3)+}(p, n, m)}{\gamma_{p,m}^+} - \frac{B_5^{(3)-}(p, n, m)}{\gamma_{m,p}^-} \right) \\
f_{i_{10}}^{(3)}(p, n) &= -\frac{1}{2Z_{c,p}} \left(\frac{B_1^{(3)+}(p, n)}{\gamma_{p,n}^-} + \frac{B_1^{(3)-}(p, n)}{\gamma_{p,n}^+} \right) \\
f_{i_{11}}^{(3)}(p, n) &= -\frac{1}{2Z_{c,p}} \left(\frac{B_2^{(3)+}(p, n)}{\gamma_{p,n}^+} - \frac{B_2^{(3)-}(p, n)}{\gamma_{n,p}^-} \right) \\
f_{i_{6 \sim 9}}^{(3)}(p) &= 0, \quad f_{i_{12 \sim 13}}^{(3)}(p, n) = 0. \tag{55}
\end{aligned}$$

2) If $(\gamma_p \neq \gamma_n)$ and $(\gamma_p = \gamma_m)$:

$$\begin{aligned}
f_{v_1}^{(3)}(p) &= \frac{1}{2} \left\{ (w_p^{(3)}(0))_+ - \frac{f_v(p) + Z_{c,p} f_i(p)}{\gamma_p - jk \cos \psi \cos \phi} \right. \\
&\quad \left. + \sum_{\substack{n=1 \\ n \neq p}}^N \left[\frac{B_1^{(3)+}(p, n)}{\gamma_{p,n}^-} + \frac{B_2^{(3)+}(p, n)}{\gamma_{p,n}^+} \right. \right. \\
&\quad \left. \left. + \frac{B_3^{(3)+}(p, n)}{\gamma_p - jk \cos \psi \cos \phi} \right. \right. \\
&\quad \left. \left. + \frac{B_4^{(3)+}(p, n)}{\gamma_{p,n}^-} + \frac{B_2^{(3)+}(p, n)}{\gamma_{p,n}^+} \right] \right\}
\end{aligned}$$

$$\begin{aligned}
& + \frac{B_3^{(3)+}(p, n)}{\gamma_p - jk \cos \psi \cos \phi} \\
& + \sum_{\substack{m=1 \\ m \neq n}}^N \left(\frac{B_5^{(3)+}(p, n, m)}{\gamma_{p,m}^+} \right) \Bigg] \Bigg\} \\
f_{v_2}^{(3)}(p) & = \frac{1}{2} \left\{ (w_p^{(3)}(d))_- e^{-\gamma_p d} \right. \\
& + \frac{f_v(p) - Z_{c,p} f_i(p)}{\gamma_p + jk \cos \psi \cos \phi} e^{-(\gamma_p + jk \cos \psi \cos \phi)d} \\
& + \sum_{\substack{n=1 \\ n \neq p}}^N \left[B_1^{(3)-}(p, n) K_{p-,n-} \right. \\
& + B_2^{(3)-}(p, n) K_{n+,p-} + B_3^{(3)-}(p, n) K_{p-} \\
& + \sum_{\substack{m=1 \\ m \neq n}}^N \left(B_4^{(3)-}(p, n, m) K_{p-,m-} - B_5^{(3)-} \right. \\
& \quad \times (p, n, m) d \Bigg) \Bigg] \Bigg\} \\
f_{v_4}^{(3)}(p, n, m) & = \frac{-B_4^{(3)-}(p, n, m)}{2\gamma_{m,p}^+} \\
f_{v_5}^{(3)}(p, n, m) & = \frac{-B_5^{(3)+}(p, n, m)}{2\gamma_{p,m}^+} \\
f_{v_6}^{(3)}(p) & = \frac{1}{2} \sum_{\substack{n=1 \\ n \neq p}}^N \sum_{\substack{m=1 \\ m \neq n}}^N B_4^{(3)+}(p, n, m) \\
f_{v_7}^{(3)}(p) & = -\frac{1}{2} \sum_{\substack{n=1 \\ n \neq p}}^N \sum_{\substack{m=1 \\ m \neq n}}^N B_5^{(3)-}(p, n, m) \\
f_{v_{10}}^{(3)}(p, n) & = -\frac{1}{2} \left(\frac{B_1^{(3+}(p, n)}{\gamma_{p,n}^-} - \frac{B_1^{(3)-}(p, n)}{\gamma_{p,n}^+} \right) \\
f_{v_{11}}^{(3)}(p, n) & = -\frac{1}{2} \left(\frac{B_2^{(3)+}(p, n)}{\gamma_{p,n}^+} + \frac{B_2^{(3)-}(p, n)}{\gamma_{n,p}^-} \right) \\
f_{v_{8-9}}^{(3)}(p) & = 0, \quad f_{v_{12-13}}^{(3)}(p, n) = 0 \\
f_{i_1}^{(3)}(p) & = \frac{f_{v_1}^{(3)}(p)}{Z_{c,p}}, \quad f_{i_2}^{(3)}(p) = -\frac{f_{v_2}^{(3)}(n)}{Z_{c,p}} \\
f_{i_4}^{(3)}(p, n, m) & = -\frac{0.5}{Z_{c,p}} \frac{B_4^{(3)+}(p, n, m)}{\gamma_{p,m}^-} \\
f_{i_5}^{(3)}(p, n, m) & = \frac{0.5}{Z_{c,p}} \frac{B_5^{(3)-}(p, n, m)}{\gamma_{m,p}^-} \\
f_{i_6}^{(3)}(p) & = \frac{0.5}{Z_{c,p}} \sum_{\substack{n=1 \\ n \neq p}}^N \sum_{\substack{m=1 \\ m \neq n}}^N B_4^{(3)+}(p, n, m)
\end{aligned}
\tag{56}$$

$$\begin{aligned}
f_{i_7}^{(3)}(p) & = \frac{0.5}{Z_{c,p}} \sum_{\substack{n=1 \\ n \neq p}}^N \sum_{\substack{m=1 \\ m \neq n}}^N B_5^{(3)-}(p, n, m) \\
f_{i_{10}}^{(3)}(p, n) & = -\frac{0.5}{Z_{c,p}} \left(\frac{B_1^{(3)+}(p, n)}{\gamma_{p,n}^+} + \frac{B_1^{(3)-}(p, n)}{\gamma_{p,n}^+} \right) \\
f_{i_{11}}^{(3)}(p, n) & = -\frac{0.5}{Z_{c,p}} \left(\frac{B_2^{(3)+}(p, n)}{\gamma_{p,n}^+} - \frac{B_2^{(3)-}(p, n)}{\gamma_{n,p}^-} \right) \\
f_{i_{8-9}}^{(3)}(p) & = 0, \quad f_{i_{12-13}}^{(3)}(p, n) = 0
\end{aligned}
\tag{57}$$

3) If ($\gamma_p = \gamma_n$) and ($\gamma_p \neq \gamma_m$):

$$\begin{aligned}
f_{v_1}^{(3)}(p) & = \frac{1}{2} \left\{ (w_p^{(3)}(0))_+ - \frac{f_v(p) + Z_{c,p} f_i(p)}{\gamma_p - jk \cos \psi \cos \phi} \right. \\
& + \sum_{\substack{n=1 \\ n \neq p}}^N \left[\frac{B_2^{(3)+}(p, n)}{\gamma_{p,n}^+} + \frac{B_3^{(3)+}(p, n)}{\gamma_p - jk \cos \psi \cos \phi} - \frac{B_7^{(3)+}(p)}{(\gamma_{p,n}^+)^2} \right. \\
& \quad \left. \left. + \sum_{\substack{m=1 \\ m \neq n}}^N \left(\frac{B_4^{(3)+}(p, n, m)}{\gamma_{p,m}^-} + \frac{B_5^{(3)+}(p, n, m)}{\gamma_{p,m}^+} \right) \right] \right\} \\
f_{v_2}^{(3)}(p) & = \frac{1}{2} \left\{ (w_p^{(3)}(d))_- e^{-\gamma_p d} \right. \\
& + \frac{f_v(p) - Z_{c,p} f_i(p)}{\gamma_p + jk \cos \psi \cos \phi} e^{-(\gamma_p + jk \cos \psi \cos \phi)d} \\
& + \sum_{\substack{n=1 \\ n \neq p}}^N \left[B_1^{(3)-}(p, n) K_{p-,n-} \right. \\
& + B_2^{(3)-}(p, n) d + B_3^{(3)-}(p, n) K_{p-} - B_6^{(3)-}(p, n) \\
& - B_6^{(3)-}(p, n) \left(\frac{de^{-\gamma_{p,n}^+ d}}{\gamma_{p,n}^+} + \frac{e^{-\gamma_{p,n}^+ d}}{(\gamma_{p,n}^+)^2} \right) + \frac{1}{2} d^2 B_7^{(3)-}(p, n) \\
& \quad \left. \left. + \sum_{\substack{m=1 \\ m \neq n}}^N \left(B_4^{(3)-}(p, n, m) K_{p-,m-} - B_5^{(3)-}(p, n, m) K_{m+,p-} \right) \right] \right\} \\
f_{v_4}^{(3)}(p, n, m) & = -\frac{1}{2} \left(\frac{B_4^{(3)+}(p, n, m)}{\gamma_{m,p}^-} - \frac{B_4^{(3)-}(p, n, m)}{\gamma_{m,p}^+} \right) \\
f_{v_5}^{(3)}(p, n, m) & = -\frac{1}{2} \left(\frac{B_5^{(3)+}(p, n, m)}{\gamma_{p,m}^+} + \frac{B_5^{(3)-}(p, n, m)}{\gamma_{p,m}^-} \right) \\
f_{v_6}^{(3)}(p) & = -\frac{1}{2} \sum_{\substack{n=1 \\ n \neq p}}^N B_1^{(3)+}(p, n), \quad f_{v_7}^{(3)}(p) = -\frac{1}{2} \sum_{\substack{n=1 \\ n \neq p}}^N B_2^{(3)-}(p, n) \\
f_{v_8}^{(3)}(p) & = -\frac{1}{4} \sum_{\substack{n=1 \\ n \neq p}}^N B_6^{(3)+}(p, n), \quad f_{v_9}^{(3)}(p) = -\frac{1}{4} \sum_{\substack{n=1 \\ n \neq p}}^N B_7^{(3)-}(p, n)
\end{aligned}$$

$$\begin{aligned}
f_{v_{10}}^{(3)}(p, n) &= \frac{1}{2} \left(\frac{B_1^{(3)-}(p, n)}{\gamma_{p,n}^+} + \frac{B_6^{(3)-}(p, n)}{(\gamma_{p,n}^+)^2} \right) \\
f_{v_{11}}^{(3)}(p, n) &= -\frac{1}{2} \left(\frac{B_2^{(3)+}(p, n)}{\gamma_{p,n}^+} + \frac{B_7^{(3)+}(p, n)}{(\gamma_{p,n}^+)^2} \right) \\
f_{v_{12}}^{(3)}(p, n) &= -\frac{1}{2} \left(B_1^{(3)+}(p, n) + \frac{B_6^{(3)-}(p, n)}{\gamma_{p,n}^+} \right) \\
f_{v_{13}}^{(3)}(p, n) &= -\frac{1}{2} \left(\frac{B_7^{(3)+}(p, n)}{\gamma_{p,n}^+} + B_2^{(3)-}(p, n) \right)
\end{aligned} \tag{58}$$

$$\begin{aligned}
f_{i_1}^{(3)}(p) &= \frac{f_{v_1}^{(3)}(p)}{Z_{c,p}}, \quad f_{i_2}^{(3)}(p) = -\frac{f_{v_2}^{(3)}(n)}{Z_{c,p}} \\
f_{i_4}^{(3)}(p, n, m) &= -\frac{0.5}{Z_{c,p}} \left(\frac{B_4^{(3)+}(p, n, m)}{\gamma_{p,m}^-} + \frac{B_4^{(3)-}(p, n, m)}{\gamma_{p,m}^+} \right) \\
f_{i_5}^{(3)}(p, n, m) &= -\frac{0.5}{Z_{c,p}} \left(\frac{B_5^{(3)+}(p, n, m)}{\gamma_{p,m}^+} - \frac{B_5^{(3)-}(p, n, m)}{\gamma_{m,p}^-} \right) \\
f_{i_6}^{(3)}(p) &= -\frac{0.5}{Z_{c,p}} \sum_{\substack{n=1 \\ n \neq p}}^N B_1^{(3)+}(p, n) \\
f_{i_7}^{(3)}(p) &= \frac{0.5}{Z_{c,p}} \sum_{\substack{n=1 \\ n \neq p}}^N B_2^{(3)-}(p, n) \\
f_{i_8}^{(3)}(p) &= -\frac{0.25}{Z_{c,p}} \sum_{\substack{n=1 \\ n \neq p}}^N B_6^{(3)+}(p, n) \\
f_{i_9}^{(3)}(p) &= \frac{0.25}{Z_{c,p}} \sum_{\substack{n=1 \\ n \neq p}}^N B_7^{(3)-}(p, n) \\
f_{i_{10}}^{(3)}(p, n) &= -\frac{0.5}{Z_{c,p}} \left(\frac{B_1^{(3)-}(p, n)}{\gamma_{p,n}^+} + \frac{B_6^{(3)-}(p, n)}{(\gamma_{p,n}^+)^2} \right) \\
f_{i_{11}}^{(3)}(p, n) &= -\frac{0.5}{Z_{c,p}} \left(\frac{B_2^{(3)+}(p, n)}{\gamma_{p,n}^+} + \frac{B_7^{(3)+}(p, n)}{(\gamma_{p,n}^+)^2} \right) \\
f_{i_{12}}^{(3)}(p, n) &= -\frac{0.5}{Z_{c,p}} \left(B_1^{(3)+}(p, n) - \frac{B_6^{(3)-}(p, n)}{\gamma_{p,n}^+} \right) \\
f_{i_{13}}^{(3)}(p, n) &= -\frac{0.5}{Z_{c,p}} \left(\frac{B_7^{(3)+}(p, n)}{\gamma_{p,n}^+} - B_2^{(3)-}(p, n) \right)
\end{aligned} \tag{59}$$

4) If ($\gamma_p = \gamma_n$) and ($\gamma_p = \gamma_m$):

$$\begin{aligned}
f_{v_1}^{(3)}(p) &= \frac{1}{2} \left\{ (w_p^{(3)}(0))_+ - \frac{f_v(p) + Z_{c,p} f_i(p)}{\gamma_p - jk \cos \psi \cos \phi} \right. \\
&\quad \left. + \sum_{\substack{n=1 \\ n \neq p}}^N \left[\frac{B_2^{(3)+}(p, n)}{\gamma_{p,n}^+} + \frac{B_3^{(3)+}(p, n)}{\gamma_p - jk \cos \psi \cos \phi} - \frac{B_7^{(3)+}(p)}{(\gamma_{p,n}^+)^2} \right] \right\}
\end{aligned}$$

$$\begin{aligned}
&+ \sum_{\substack{m=1 \\ m \neq n}}^N \left(\frac{B_5^{(3)+}(p, n, m)}{\gamma_{p,m}^+} \right) \Big] \Big\} \\
f_{v_2}^{(3)}(p) &= \frac{1}{2} \left\{ (w_p^{(3)}(d))_- e^{-\gamma_p d} \right. \\
&\quad + \frac{f_v(p) - Z_{c,p} f_i(p)}{\gamma_p + jk \cos \psi \cos \phi} e^{-(\gamma_p + jk \cos \psi \cos \phi)d} \\
&\quad + \sum_{\substack{n=1 \\ n \neq p}}^N \left[B_1^{(3)-}(p, n) K_{p-,n} - \right. \\
&\quad \left. + B_2^{(3)-}(p, n) d + B_3^{(3)-}(p, n) K_{p-} - B_6^{(3)-}(p, n) \right. \\
&\quad \left. - B_6^{(3)-}(p, n) \left(\frac{de^{-\gamma_{p,n}^+ d}}{\gamma_{p,n}^+} + \frac{e^{-\gamma_{p,n}^+ d}}{(\gamma_{p,n}^+)^2} \right) + \frac{1}{2} d^2 B_7^{(3)-}(p, n) \right. \\
&\quad \left. + \sum_{\substack{m=1 \\ m \neq n}}^N \left(B_4^{(3)-}(p, n, m) K_{p-,m} - B_5^{(3)-}(p, n, m) d \right) \right] \Big\} \\
f_{v_4}^{(3)}(p, n, m) &= -\frac{1}{2} \left(-\frac{B_4^{(3)-}(p, n, m)}{\gamma_{m,p}^+} \right) \\
f_{v_5}^{(3)}(p, n, m) &= -\frac{1}{2} \left(\frac{B_5^{(3)+}(p, n, m)}{\gamma_{p,m}^+} \right) \\
f_{v_6}^{(3)}(p) &= -\frac{1}{2} \sum_{\substack{n=1 \\ n \neq p}}^N \left(B_1^{(3)+}(p, n) + \sum_{\substack{m=1 \\ m \neq n}}^N B_4^{(3)+}(p, n, m) \right) \\
f_{v_7}^{(3)}(p) &= -\frac{1}{2} \sum_{\substack{n=1 \\ n \neq p}}^N \left(B_2^{(3)-}(p, n) + \sum_{\substack{m=1 \\ m \neq n}}^N B_5^{(3)-}(p, n, m) \right) \\
f_{v_8}^{(3)}(p) &= -\frac{1}{4} \sum_{\substack{n=1 \\ n \neq p}}^N B_6^{(3)+}(p, n), \quad f_{v_9}^{(3)}(p) = -\frac{1}{4} \sum_{\substack{n=1 \\ n \neq p}}^N B_7^{(3)-}(p, n) \\
f_{v_{10}}^{(3)}(p, n) &= \frac{1}{2} \left(\frac{B_1^{(3)-}(p, n)}{\gamma_{p,n}^+} + \frac{B_6^{(3)-}(p, n)}{(\gamma_{p,n}^+)^2} \right) \\
f_{v_{11}}^{(3)}(p, n) &= -\frac{1}{2} \left(\frac{B_2^{(3)+}(p, n)}{\gamma_{p,n}^+} + \frac{B_7^{(3)+}(p, n)}{(\gamma_{p,n}^+)^2} \right) \\
f_{v_{12}}^{(3)}(p, n) &= -\frac{1}{2} \left(B_1^{(3)+}(p, n) + \frac{B_6^{(3)-}(p, n)}{\gamma_{p,n}^+} \right) \\
f_{v_{13}}^{(3)}(p, n) &= -\frac{1}{2} \left(\frac{B_7^{(3)+}(p, n)}{\gamma_{p,n}^+} + B_2^{(3)-}(p, n) \right) \\
f_{i_1}^{(3)}(p) &= \frac{f_{v_1}^{(3)}(p)}{Z_{c,p}}, \quad f_{i_2}^{(3)}(p) = -\frac{f_{v_2}^{(3)}(n)}{Z_{c,p}} \\
f_{i_4}^{(3)}(p, n, m) &= -\frac{0.5}{Z_{c,p}} \left(+ \frac{B_4^{(3)-}(p, n, m)}{\gamma_{p,m}^+} \right)
\end{aligned}$$

$$\begin{aligned}
f_{i_5}^{(3)}(p, n, m) &= -\frac{0.5}{Z_{c,p}} \left(\frac{B_5^{(3)+}(p, n, m)}{\gamma_{p,m}^+} \right) \\
f_{i_6}^{(3)}(p) &= -\frac{0.5}{Z_{c,p}} \sum_{\substack{n=1 \\ n \neq p}}^N \left(B_1^{(3)+}(p, n) + \sum_{\substack{m=1 \\ m \neq n}}^N B_4^{(3)+}(p, n, m) \right) \\
f_{i_7}^{(3)}(p) &= \frac{0.5}{Z_{c,p}} \sum_{\substack{n=1 \\ n \neq p}}^N \left(B_2^{(3)-}(p, n) + \sum_{\substack{m=1 \\ m \neq n}}^N B_5^{(3)-}(p, n, m) \right) \quad (60) \\
f_{i_8}^{(3)}(p) &= -\frac{0.25}{Z_{c,p}} \sum_{\substack{n=1 \\ n \neq p}}^N B_6^{(3)+}(p, n) \\
f_{i_9}^{(3)}(p) &= \frac{0.25}{Z_{c,p}} \sum_{\substack{n=1 \\ n \neq p}}^N B_7^{(3)-}(p, n) \\
f_{i_{10}}^{(3)}(p, n) &= -\frac{0.5}{Z_{c,p}} \left(\frac{B_1^{(3)-}(p, n)}{\gamma_{p,n}^+} + \frac{B_6^{(3)-}(p, n)}{(\gamma_{p,n}^+)^2} \right) \\
f_{i_{11}}^{(3)}(p, n) &= -\frac{0.5}{Z_{c,p}} \left(\frac{B_2^{(3)+}(p, n)}{\gamma_{p,n}^+} + \frac{B_7^{(3)+}(p, n)}{(\gamma_{p,n}^+)^2} \right) \\
f_{i_{12}}^{(3)}(p, n) &= -\frac{0.5}{Z_{c,p}} \left(B_1^{(3)+}(p, n) - \frac{B_6^{(3)-}(p, n)}{\gamma_{p,n}^+} \right) \\
f_{i_{13}}^{(3)}(p, n) &= -\frac{0.5}{Z_{c,p}} \left(\frac{B_7^{(3)+}(p, n)}{\gamma_{p,n}^+} - B_2^{(3)-}(p, n) \right) \quad (61)
\end{aligned}$$

REFERENCES

- [1] C. R. Paul, *Analysis of Multiconductor Transmission Lines*, 2nd ed. the New York, USA: Wiley, 2008.
- [2] F. M. Tesche, M. V. Ianoz, and T. Karlsson, *EMC Analysis Methods and Computational Models*. New York, USA: Wiley, 1997.
- [3] C. R. Paul, “Solution of the transmission-line equations under the weak-coupling assumption,” *IEEE Trans. Electromagn. Compat.*, vol. 44, no. 3, pp. 413–423, Aug. 2002.
- [4] F. Canavero and I. Maio, “Transient simulation of lossy multiconductor interconnects,” in *Proc. 1997 Int. Symp. Electromagn. Compat.*, May 21–23, 1997, pp. 243–246.
- [5] C. R. Paul, “Computation of crosstalk in a multiconductor transmission line,” *IEEE Trans. Electromagn. Compat.*, vol. EMC-23, no. 4, pp. 352–358, Nov. 1981.
- [6] C. R. Paul, “Literal solutions for time-domain crosstalk on lossless transmission lines,” *IEEE Trans. Electromagn. Compat.*, vol. 34, no. 4, pp. 433–444, Nov. 1992.
- [7] R. Achar and M. S. Nakhla, “Simulation of high-speed interconnects,” in *Proc. IEEE*, May 2001, vol. 89, no. 5, pp. 693–728.
- [8] N. Nakhla, A. Ruehli, M. Nakhla, and R. Achar, “Simulation of coupled interconnects using waveform relaxation and transverse partitioning,” in *Proc. IEEE 13th Topical Meet. Electr. Performance Electron. Packag.*, Oct. 2004, pp. 25–28.
- [9] N. Nakhla, A. E. Ruehli, M. S. Nakhla, R. Achar, and C.-Z. Chen, “Waveform relaxation techniques for simulation of coupled interconnects with frequency-dependent parameters,” *IEEE Trans. Adv. Packag.*, vol. 30, no. 2, pp. 257–269, Feb. 2007.
- [10] Y.-Z. Xie, F. Canavero, T. Maextri, and Z.-J. Wang, “Crosstalk analysis of multiconductor transmission lines based on distributed analytical representation and iterative technique,” *IEEE Trans. Electromagn. Compat.*, vol. 52, no. 3, pp. 712–727, Aug. 2010.
- [11] I. M. Elfadel, “Convergence of transverse waveform relaxation for the electrical analysis of very wide transmission line buses,” *IEEE Trans. Comput.-Aided Des. Integr. Circuits Syst.*, vol. 28, no. 8, pp. 1150–1161, Aug. 2009.
- [12] Electromagnetic compatibility—Part 2: Environment, Section IX:Description of HEMP environment-Radiated disturbance, 1996.
- [13] M. A. Farhan, N. M. Nakhla, M. S. Nakhla, R. Achar, and A. E. Ruehli, “Overlapping partitioning techniques for simulation of strongly coupled distributed interconnects,” *IEEE Trans. Components, Packag. Manufact. Technol.*, vol. 2, no. 7, pp. 1193–1201, Jul. 2012.
- [14] F. Rachidi and S. V. Tkachenko, *Electromagnetic Field Interaction With Transmission Lines, From Classical Theory to HF Radiation Effects*. Southampton, U.K.: WIT PRESS, 2008.
- [15] C. E. Baum, T. K. Liu, and F. M. Tesche, “On the analysis of general multiconductor transmission line networks,” *Interaction Note* 350, 1978.
- [16] N. Nakhla, A. Ruehli, M. S. Nakhla, and R. Achar, “Simulation of coupled interconnects using waveform relaxation and transverse partitioning,” *IEEE Trans. Adv. Packag.*, vol. 29, no. 1, pp. 78–87, Feb. 2006.
- [17] A. R. Sridhar, N. M. Nakhla, R. Achar, M. S. Nakhla, and A. E. Ruehli, “Fast EMI analysis via transverse partitioning and waveform relaxation,” *IEEE Trans. Electromagn. Compat.*, vol. 51, no. 2, pp. 358–371, May 2009.
- [18] G. S. Shinh, N. M. Nakhla, R. Achar, M. S. Nakhla, A. Dounavis, and I. Erdin, “Fast transient analysis of incident field coupling to multiconductor transmission lines,” *IEEE Trans. Electromagn. Compat.*, vol. 48, no. 1, pp. 57–73, Feb. 2006.
- [19] F. M. Tesche, “Development and use of the BLT equation in the time domain as applied to a coaxial cable,” *IEEE Trans. Electromagn. Compat.*, vol. 49, no. 1, pp. 3–11, Feb. 2007.
- [20] A. Dounavis, R. Achar, and M. S. Nakhla, “A general class of passive macromodels for lossy multiconductor transmission lines,” *IEEE Trans. Microw. Theor. Tech.*, vol. 49, no. 10, pp. 1686–1696, Oct. 2001.
- [21] Y.-Z. XIE, F. Canavero, T. Maestri, and Wang Zan-ji, “Analytic iterative approach to crosstalk analysis of multiconductor transmission lines,” in *Proc. Eur. Electromagn. Compat.*, 2010, pp. 775–780.